ISSN 1070-3632, Russian Journal of General Chemistry, 2014, Vol. 84, No. 6, pp. 1157–1178. © Pleiades Publishing, Ltd., 2014.
Original Russian Text © A.T. Gubaidullin, V.N. Nabiullin, S.V. Kharlamov, B.I. Buzykin, 2014, published in Zhurnal Obshchei Khimii, 2014, Vol. 84, No. 6, pp. 977–999.

# Tautomerism of Aza Heterocycles: V.[1] Structure of the Spontaneous Transformation Products of 5-Methyl-2-phenyl-3,3a,4,5,6,7-hexahydro-2*H*-pyrazolo-[4,3-*c*]pyridin-3-one in Crystal and Solution

**A. T. Gubaidullin, V. N. Nabiullin, S. V. Kharlamov, and B. I. Buzykin**

*Arbuzov Institute of Organic and Physical Chemistry, Kazan Scientific Center, Russian Academy of Sciences, ul. Arbuzova 8, Kazan, 420088 Tatarstan, Russia*
*e-mail: buz@iopc.ru*

Received June 17, 2013

**Abstract**—5-Methyl-2-phenyl-3,3a,4,5,6,7-hexahydro-2*H*-pyrazolo[4,3-*c*]pyridin-3-one exists as zwitterion with a proton localized on the nitrogen atom of the piperidine ring and negative charge delocalized over the pyrazololate fragment. The compound is stable in crystal but ustable in solution. Its chromatographic purification and attempts to recrystallize or synthesize by condensation of phenylhydrazine with alkyl 1-methyl-4-oxopiperidin-3-carboxylate on heating in alcohols or benzene lead to the formation of a complex mixture of products. Among these products, we isolated and identified 3a,3a′-methylenebis(5-methyl-2-phenyl-3,3a,4,5,6,7-hexahydro-2*H*-pyrazolo[4,3-*c*]pyridin-3-one), 1-methyl-3-(2-phenylhydrazinylidene)pyrrolidin-2-one, and 5-methyl-2-phenyl-3,5,6,7-tetrahydro-2*H*-pyrazolo[4,3-*c*]pyridine. The structure of methyl 3-(2-phenylhydrazinylidene)-4,5-dihydro-3*H*-pyrrole-2-carboxylate and 3a,5-dimethyl-2-phenyl-3,3a,4,5,6,7-hexahydro-2*H*-pyrazolo[4,3-*c*]pyridin-3-one was proved by NMR spectroscopy. 3a,5-Dimethyl-2-phenyl-3,3a,4,5,6,7-hexahydro-2*H*-pyrazolo[4,3-*c*]pyridin-3-one was isolated as hydrochloride hydrate whose structure was determined by X-ray analysis.

**Keywords:** aza cycles, dihydropyrazolone, pyrrolidin-2-one, dihydropyrrole, autoalkylation, X-ray analysis

**DOI:** 10.1134/S1070363214060188

In the preceding communication [1] we showed that condensation products of phenylhydrazine with alkyl 1-alkyl-4-oxopiperidin-3-carboxylates **Ia**–**Ic** (R = Me, Et) are not conventional CH (**IIa**), NH, or OH tautomers of pyrazolone fused at the $C^3$–$C^4$ bond to piperidine ring. We found that 5-methyl-2-phenyl-3,3a,4,5,6,7-hexahydro-2*H*-pyrazolo[4,3-*c*]pyridin-3-one (**IIa**) in crystal exists as zwitterion **IV** with protonated nitrogen atom of the piperidine ring and delocalization of the negative charge over the pyrazololate fragment; structure **IV** is more favorable than that with negative charge localization on the oxygen (structure **III**) or $N^1$ nitrogen atom of the pyrazole ring [1] (Scheme 1).

We failed to determine whether structure **IV** is the only one existing in solution of pyrazolopiperidine **IIa** or equilibrium between zwitterionic forms **III** and **IV** and CH, OH, and $N^1$H tautomers is possible. The reason is that compound **IIa** is almost insoluble in nonpolar solvents and is unstable in polar solvents ($H_2O$, AcOH, $CF_3COOH$, DMSO) and even in those solvents where it is poorly soluble (alcohols, benzene, etc.). Crystalline pyrazolopiperidine (**IIa**) can be stored for many years without appreciable change (according to the IR data). Dissolution of **IIa** in alcohols and benzene and subsequent storage of these solutions leads to formation of the same complex mixtures of products as those obtained on attempted synthesis of **IIa** in boiling solvents. The transformation of **IIa** in solution is especially fast at elevated temperature. Chromatographic purification or recrystallization of **IIa** from alcohols (MeOH, EtOH, *i*-PrOH), benzene, or other solvents results in its complete transformation into a mixture of compounds **V**–**IX** and some others.

[1] For communication IV, see [1].

**Scheme 1.**

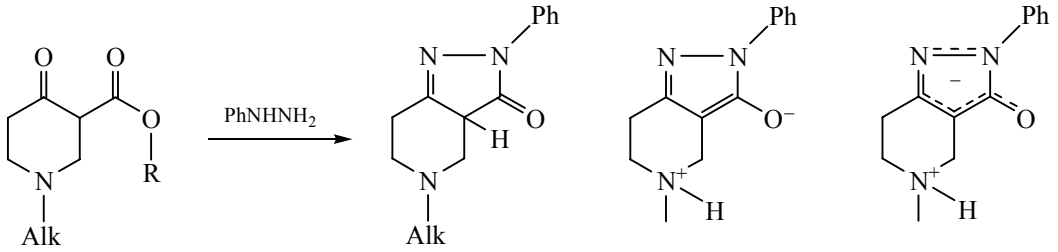


**Ia–Ic** **IIa–IIc** **III** **IV**

Alk = Me (**Ia, IIa**), Et (**Ib, IIb**), Pr (**Ic, IIc**); R = Me or Et.

**Scheme 2.**

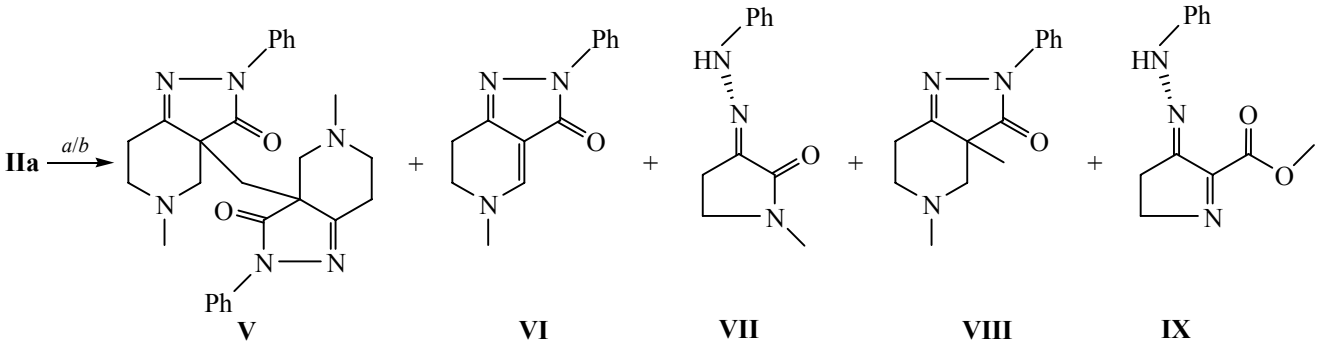


**V** **VI** **VII** **VIII** **IX**

*a*, MeOH, 65°C; *b*, *i*-PrOH, 80°C.

We succeeded in isolating and unambiguously identifying 3a,3a′-methylenebis(5-methyl-2-phenyl-3,3a,4,5,6,7-hexahydro-2*H*-pyrazolo[4,3-*c*]pyridin-3-one) (**V**) [2, 3], 1-methyl-3-(2-phenylhydrazinylidene)-pyrrolidin-2-one (**VII**), and 5-methyl-2-phenyl-3,5,6,7-tetrahydro-2*H*-pyrazolo[4,3-*c*]pyridine (**VI**) [3–6]. By NMR spectroscopy we also determined the structure of methyl 3-(2-phenylhydrazinylidene)-4,5-dihydr-3*H*-pyrrole-2-carboxylate (**IX**) and 3a,5-dimethyl-2-phenyl-3,3a,4,5,6,7-hexahydro-2*H*-pyrazolo[4,3-*c*]-pyridin-3-one (**VIII**) [7] (Scheme 2).

In the reaction of phenylhydrazine with keto ester **Ia** (R = Me) under standard conditions of synthesis of pyrazol-5-ones (heating of the reactants in alcohols or benzene) we observed formation of a complex mixture of 5–7 compounds among which no pyrazolopiperidine **IIa** was detected [2–6]. When a mixture of **Ia** and phenylhydrazine in methanol, propan-2-ol, or benzene was heated for 5 min under reflux, the products were compounds **V**, **VI**, *E* isomer of hydrazonopyrrolidine **VII**, and some other compounds, but there was no pyrazolopiperidine **IIa**. Dihetarylmethane **V** and pyrazolotetrahydropyridine **VI** always predominated among the products. The latter was formed in high yield, e.g., when pyrazolopiperidine **IIa** was dissolved in DMSO. In all cases, the amount of hydrazonopyrrolidine **VII** was considerably smaller. These three major products were isolated as pure substances and were extensively studied by spectral methods; moreover, we succeeded in obtaining their single crystals suitable for X-ray analysis. Later, we also succeeded in detecting 3a,5-dimethyl-2-phenyl-3,3a,4,5,6,7-hexahydro-2*H*-pyrazolo[4,3-*c*]pyridin-3-one (**VIII**) and methyl (*E*)-3-(2-phenylhydrazinylidene)-4,5-dihydro-3*H*-pyrrole-2-carboxylate (**IX**) [7]. Some other products in such reaction mixtures were detected only by thin-layer chromatography.

As we showed previously [1, 7], pyrazolopiperidine **IIa** is a multident base which forms three hydrochlorides **X**–**XII** differing by the acid–base ratio: sesquihydrochloride **X** (2**IIa**·3HCl), hemihydrochloride **XI** (2**IIa**·HCl), and dichloride **XII** (**IIa**·2HCl). Hydrochlorides **X**–**XII** are stable compounds which can be stored for many years without appreciable change; however, we failed to isolate free base **IIa** from any salt **X**–**XII**. In all cases, the

**Scheme 3.**

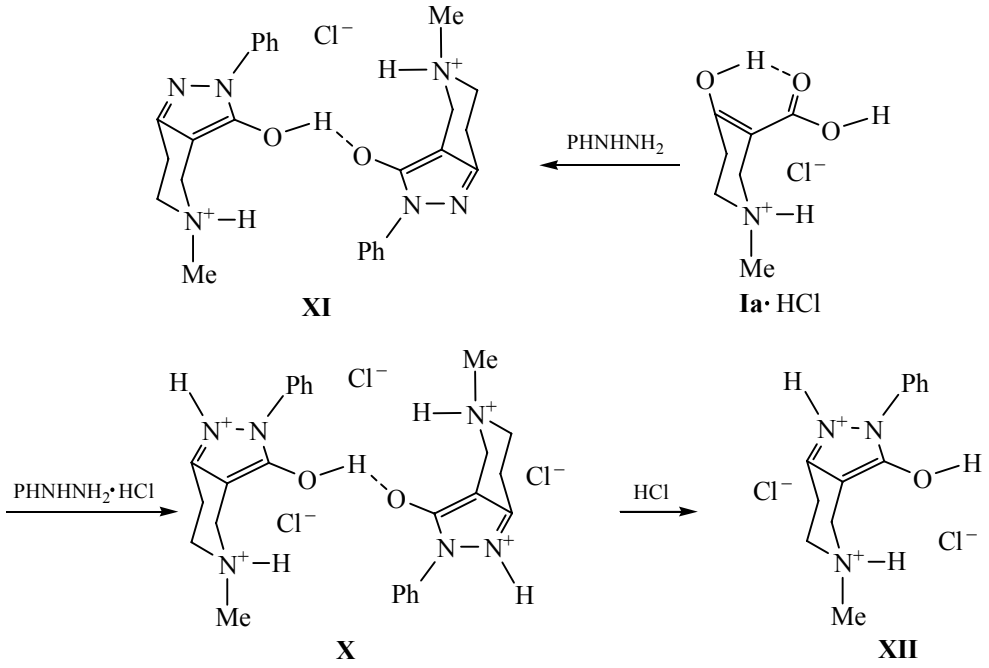


formation of complex mixtures of products **V**–**IX** and others was observed, and their ratio depended on the isolation conditions [3, 5–7] (Scheme 3).

The structure of products **V**–**VII** was confirmed by their elemental compositions, IR and mass spectra, and X-ray analysis, as well as by a set of one- and two-dimensional NMR correlation techniques (COSY, $^{1}H$–$^{13}C$/$^{1}H$–$^{15}N$ HSQC and HMBC) [8, 9]. The 2D DOSY and 1D DPFGNOE techniques [10, 11] were applied to determine the self-diffusion coefficients and nuclear Overhauser effects (NOE), respectively. The structure

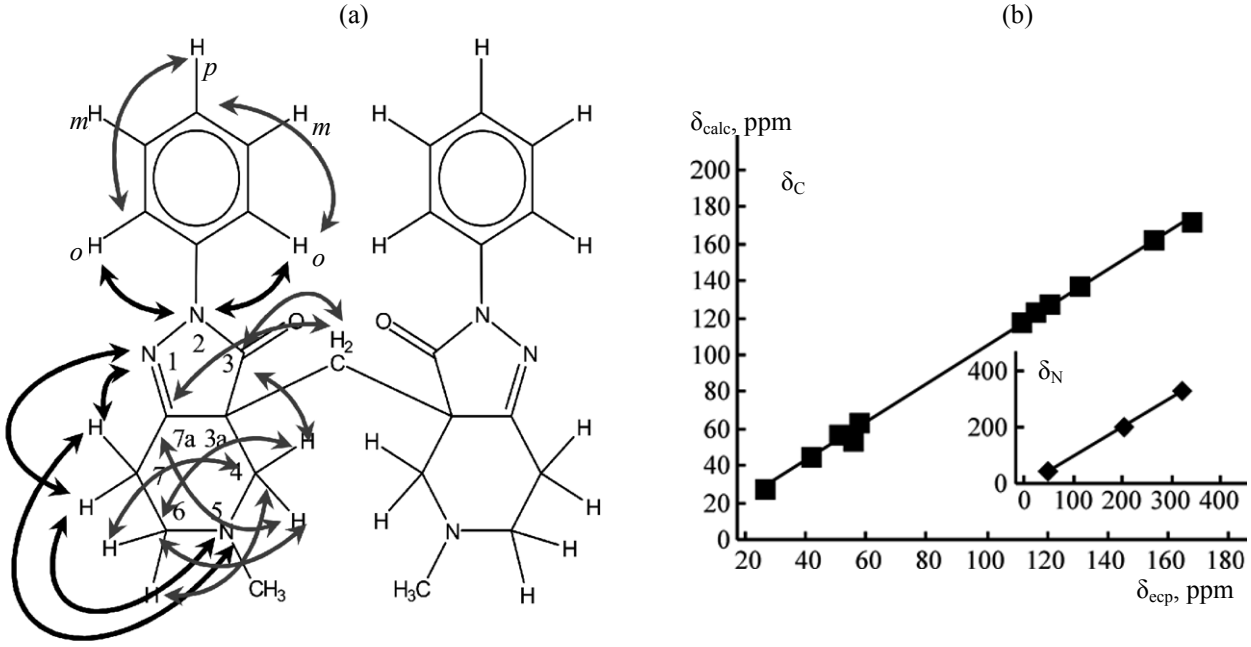


**Fig. 1.** (a) Schematic representation of $^{1}H$–$^{13}C$ (gray double-arrowed lines) and $^{1}H$–$^{15}N$ couplings (black double-arrowed lines) in the molecule of dihetarylmethane **V** and (b) correlations between the calculated and experimental $\delta_C$ and $\delta_N$ values.

**Table 1.** Selected bond lengths (Å) in molecules **V**, **VI**, and **XIII**[a]

| Bond | V1A | V1B | V2A | V2B | VIA | VIB | XIII[b] |
|---|---|---|---|---|---|---|---|
| $O^3$–$C^3$ | 1.221(2) | 1.217(2) | 1.213(4) | 1.244(5) | 1.227(3) | 1.226(3) | 1.223(2) |
| $N^1$–$N^2$ | 1.420(2) | 1.421(2) | 1.421(4) | 1.413(5) | 1.406(3) | 1.408(3) | 1.417(2) |
| $N^1$–$C^9$ | 1.276(2) | 1.282(2) | 1.283(5) | 1.301(6) | 1.301(3) | 1.302(4) | 1.284(2) |
| $N^2$–$C^3$ | 1.371(2) | 1.378(2) | 1.362(5) | 1.359(5) | 1.403(3) | 1.401(3) | 1.376(2) |
| $N^2$–$C^{10}$ | 1.420(2) | 1.417(2) | 1.426(5) | 1.422(6) | 1.408(3) | 1.407(3) | 1.416(2) |
| $N^6$–$C^5$ | 1.460(2) | 1.454(2) | 1.457(5) | 1.460(6) | 1.312(3) | 1.315(3) | 1.500(2) |
| $N^6$–$C^7$ | 1.463(2) | 1.458(2) | 1.454(6) | 1.471(6) | 1.442(4) | 1.446(4) | 1.506(2) |
| $N^6$–$C^{16}$ | 1.458(2) | 1.460(2) | 1.456(5) | 1.447(6) | 1.466(3) | 1.460(3) | 1.499(2) |
| $C^3$–$C^4$ | 1.516(2) | 1.520(2) | 1.518(5) | 1.489(6) | 1.431(3) | 1.431(3) | 1.521(3) |
| $C^4$–$C^5$ | 1.543(2) | 1.547(2) | 1.560(5) | 1.553(6) | 1.371(3) | 1.370(4) | 1.531(2) |
| $C^4$–$C^9$ | 1.497(2) | 1.495(2) | 1.482(5) | 1.490(6) | 1.405(3) | 1.402(3) | 1.500(3) |
| $C^4$–$C^{17}$ | 1.541(2) | 1.542(2) | 1.541(4) | 1.526(5) | – | – | 1.537(3) |
| $C^7$–$C^8$ | 1.527(3) | 1.529(3) | 1.526(6) | 1.502(8) | 1.483(5) | 1.401(4) | 1.530(3) |
| $C^8$–$C^9$ | 1.491(2) | 1.487(2) | 1.488(6) | 1.499(7) | 1.482(4) | 1.467(4) | 1.487(3) |

[a] The bond lengths in the benzene fragments of all compounds are close to reference values. [b] The $N^6$–$H^6$ bond length in **XIII** is 1.08(2) Å.

of dihetarylmethane **V** was established using a series of homo- and heteronuclear shift correlation experiments ($^1$H–$^1$H, $^1$H–$^{13}$C, $^1$H–$^{15}$N; Fig. 1a; trivial $^1$H–$^1$H COSY and $^1$H–$^{13}$C HSQC correlations are not shown). A good correlation ($R^2$ = 0.99) between the calculated (GIAO DFT) and experimental $^{13}$C and $^{15}$N chemical shifts (Fig. 1b) may be regarded as an additional evidence in favor of the assumed structure of **V** in solution.

Compound **V** is a dihydric base which reacts with HCl to produce dihydrochloride **V**·2HCl. Unlike pyrazolopiperidine **IIa**, free base **V** can be readily recovered from its dihydrochloride, and the latter can be stored for many years. The $^1$H NMR spectra of **V** in MeOH and MeOD are more complex than in $CCl_4$, but removal of methanol leaves unchanged compound **V**. Variation of the $^1$H NMR spectra was also observed for solutions of **V** in DMSO-$d_6$. The most stable are solutions of **V** in methylene chloride.

Compound **V** crystallizes from many solvents to give well-shaped crystals. We isolated two polymorphic modifications of **V**: monoclinic **V1** (from MeOH, EtOH, *i*-PrOH, MeCN, acetone) and rhombic **V2** (from $CH_2Cl_2$), the latter crystallizing in $P2_12_12$ chiral space group. Asymmetric parts of unit cells of polymorphs **V1** and **V2** each contain 1/2 of two molecules (**V1A**, **V1B** and **V2A**, **V2B**) which are located in partial positions on the second-order rotation axes passing through the bridging carbon atoms. The molecular structures of both polymorphs of **V** and their crystal packings are shown in Figs. 2–5, and their selected geometric parameters are given in Tables 1–3.

All four molecules of two polymorphs turned out to have the structure of a single tautomer, 3,3a,4,5,6,7-hexahydro-2*H*-pyrazolo[4,3-*c*]pyridin-3-one derivative. Hydrogen atoms of the $C^8H_2$ bridging methylene group, though constitute the $C^8$–$C^9$=$N^1$ enamine fragment, are insufficiently acidic to allow formation of $N^1$H tautomer and the more so zwitterionic structures. This conclusion is also supported by analysis of the bond lengths (Table 1). The $C^3$=$O^3$ bond lengths exactly match the double bond (1.217–1.244 Å; reference data: 1.210 Å [12]) despite the neighborhood of the $C^3$–$N^2$ amide bond. The length of

**Table 2.** Selected bond angles (ω, deg) in molecules **V**, **VI**, and **XIII**[a]

| Angle | V1A | V1B | V2A | V2B | VIA | VIB | XIII[b] |
|---|---|---|---|---|---|---|---|
| $N^1N^2C^3$ | 112.3(1) | 112.2(1) | 112.8(3) | 111.3(3) | 112.7(2) | 112.5(2) | 112.4(1) |
| $N^1N^2C^{10}$ | 118.5(1) | 118.3(1) | 118.4(3) | 117.3(4) | 118.3(2) | 118.5(2) | 119.0(1) |
| $N^2N^1C^9$ | 106.9(1) | 106.9(1) | 106.4(3) | 105.8(4) | 104.6(2) | 104.6(2) | 106.8(2) |
| $C^3N^2C^{10}$ | 129.1(2) | 129.4(1) | 128.7(3) | 131.4(4) | 128.9(2) | 129.0(2) | 127.9(2) |
| $C^5N^6C^7$ | 111.4(1) | 111.3(1) | 110.1(3) | 110.9(4) | 121.0(2) | 119.6(2) | 112.2(1) |
| $C^5N^6C^{16}$ | 109.8(1) | 111.0(1) | 109.7(4) | 109.8(4) | 122.0(2) | 123.0(2) | 109.0(1) |
| $C^7N^6C^{16}$ | 111.3(1) | 111.4(1) | 110.8(3) | 110.8(5) | 116.4(2) | 117.3(2) | 110.7(1) |
| $O^3C^3N^2$ | 127.1(1) | 126.8(1) | 128.5(3) | 124.9(4) | 125.2(2) | 125.6(2) | 127.3(2) |
| $O^3C^3C^4$ | 127.2(1) | 127.7(1) | 126.0(3) | 126.2(4) | 132.1(2) | 131.6(2) | 127.0(2) |
| $C^2C^3C^4$ | 105.7(1) | 105.5(1) | 105.5(3) | 108.9(4) | 102.7(2) | 102.9(2) | 105.6(1) |
| $C^3C^4C^5$ | 111.0(1) | 112.7(1) | 111.2(3) | 111.5(4) | 131.3(2) | 131.8(2) | 110.9(1) |
| $C^3C^4C^9$ | 100.5(1) | 100.6(1) | 100.9(3) | 98.8(4) | 106.7(2) | 106.6(2) | 100.1(1) |
| $C^3C^4C^{17}$ | 111.5(1) | 111.8(1) | 112.4(3) | 112.4(4) | – | – | 109.3(1) |
| $C^5C^4C^9$ | 106.5(1) | 106.0(1) | 105.9(3) | 106.2(4) | 121.9(2) | 121.5(2) | 109.6(1) |
| $C^5C^4C^{17}$ | 109.0(1) | 108.0(1) | 108.1(3) | 109.2(3) | – | – | 112.9(1) |
| $C^9C^4C^{17}$ | 118.1(1) | 117.6(1) | 118.1(3) | 118.4(4) | – | – | 113.3(2) |
| $N^6C^5C^4$ | 109.6(1) | 109.3(1) | 110.3(3) | 109.2(4) | 121.3(2) | 122.2(2) | 110.9(1) |
| $N^6C^7C^8$ | 111.0(1) | 110.5(1) | 111.8(3) | 111.9(4) | 117.9(2) | 121.5(3) | 110.9(1) |
| $C^7C^8C^9$ | 107.9(1) | 108.4(1) | 107.4(3) | 106.9(4) | 112.1(3) | 116.1(3) | 107.8(1) |
| $N^1C^9C^4$ | 114.1(1) | 114.2(1) | 114.2(3) | 115.1(4) | 113.3(2) | 113.4(2) | 114.2(2) |
| $N^1C^9C^8$ | 124.1(1) | 123.8(1) | 123.7(3) | 123.1(4) | 127.1(2) | 127.6(2) | 125.5(2) |
| $C^4C^9C^8$ | 120.3(1) | 120.7(1) | 120.5(3) | 120.0(4) | 119.4(2) | 118.9(2) | 119.6(2) |
| $N^2C^{10}C^{11}$ | 119.9(1) | 119. 8(1) | 120.7(4) | 119.6(5) | 120.1(2) | 119.8(2) | 119.6(2) |
| $N^2C^{10}C^{15}$ | 120.4(1) | 120.7(1) | 120.7(4) | 120.3(5) | 120.7(2) | 121.7(2) | 120.2(2) |
| $C^4C^{17}C^{4'}$ | 119.8(2) | 119.6(1) | 117.3(4) | 119.5(5) | – | – | – |

[a] The bond angles in the benzene fragments of all compounds are close to reference values. [b] Bond angles in **XIII**: $C^5N^6H^6$ 107.7(2)°, $C^7N^6H^6$ 108.6(2)°, $C^{16}N^6H^6$ 108.4(2)°.

the latter (1.276–1.307 Å) is likely to be largely determined by conjugation with the C=N bond and phenyl ring. The two independent molecules of rhombic polymorph **V2** display somewhat larger difference in the C=O bond lengths, as compared to monoclinic polymorph **V1**. The $C^9$=$N^1$, $N^1$–$N^2$, and $N^2$–$C^{10}$ bond lengths (Table 1) indicate the existence of conjugation between these fragments. Although these bonds constitute a part of the pyrazolone ring, their parameters are more typical of common phenylhydrazones [13, 14]. The C–C and N–C bond lengths in the piperidine rings approach those in saturated heterocycles [12]; only the $C^8$–$C^9$ bonds are slightly shorter due to their involvement in the enamine fragment (Table 1). The bond angles in the pyrazole and piperidine rings of molecules of both polymorphs of **V** are similar to the corresponding values for structurally related heterocycles (Table 2).

Pincer-like molecular conformations of polymorph **V2** almost do not differ in the angles of rotation of the bicyclic fragments about the bonds connecting them

**Table 3.** Selected torsion angles (φ, deg) in molecules **V**, **VI**, and **XIII**

| Angle | V1A | V1B | V2A | V2B | VIA | VIB | XIII |
|---|---|---|---|---|---|---|---|
| $N^1N^2C^3O^3$ | –173.8(1) | 173.3(1) | 174.1(3) | –175.5(4) | 177.5(3) | 179.8(3) | –171.7(2) |
| $N^1N^2C^3C^4$ | 6.5(2) | –7.7(1) | –4.5(4) | 2.9(5) | –2.1(3) | –0.3(3) | 8.8(2) |
| $N^1N^2C^{10}C^{11}$ | 15.1(2) | –12.8(2) | –4.9(6) | 4.2(7) | –6.7(3) | –0.5(4) | 16.5(3) |
| $N^1N^2C^{10}C^{15}$ | –163.6(2) | 167.4(1) | 175.2(5) | –177.1(5) | 172.6(2) | 179.5(2) | –163.1(2) |
| $N^1C^9C^4C^{17}$ | –120.3(1) | 120.5(1) | 122.7(4) | –123.0(5) | – | – | –110.8(2) |
| $N^2N^1C^9C^4$ | 2.6(2) | –3.2(2) | –2.4(4) | 3.3(5) | 0.0(3) | –0.2(3) | –0.5(2) |
| $N^2N^1C^9C^8$ | 168.7(1) | –170.4(1) | –167.8(4) | 168.1(5) | –175.6(3) | 179.0(3) | 170.1(2) |
| $N^2C^3C^4C^5$ | –116.7(1) | 117.7(1) | 114.7(3) | –112.2(4) | 179.1(3) | –179.1(2) | –123.8(2) |
| $N^2C^3C^4C^9$ | –4.5(1) | 5.2(1) | 2.8(4) | –0.9(5) | 1.9(3) | 0.2(3) | –8.1(2) |
| $N^2C^3C^4C^{17}$ | 121.5(1) | –120.4(1) | –124.0(3) | 124.8(4) | – | – | 111.1(2) |
| $N^6C^5C^4C^9$ | 54.8(1) | –55.1(1) | –54.9(4) | 55.1(5) | –6.0(4) | 0.5(4) | 48.9(2) |
| $N^6C^5C^4C^{17}$ | –73.5(1) | 71.7(1) | 72.6(4) | –73.5(4) | – | – | –78.4(2) |
| $N^6C^7C^8C^9$ | –50.3(2) | 49.6(2) | 51.6(5) | –51.8(6) | –29.7(4) | 4.3(6) | –53.5(2) |
| $O^3C^3N^2C^{10}$ | 0.2(3) | –2.9(2) | –3.4(6) | 3.8(8) | –6.2(4) | –0.3(4) | –1.3(3) |
| $O^3C^3C^4C^5$ | 63.6(2) | –63.3(2) | –63.9(5) | 66.2(6) | –0.4(5) | 0.8(5) | 56.8(3) |
| $O^3C^3C^4C^9$ | 175.8(1) | –175.8(2) | –175.9(3) | 177.5(4) | –177.6(3) | 180.0(3) | 172.5(2) |
| $O^3C^3C^4C^{17}$ | –58.2(2) | 58.6(2) | 57.3(5) | –56.8(6) | – | – | –68.3(2) |
| $C^3N^2N^1C^9$ | –6.0(2) | 7.1(2) | 4.5(4) | –3.9(5) | 1.4(3) | 0.3(3) | –5.6(2) |
| $C^3N^2C^{10}C^{11}$ | –160.4(1) | 163.2(1) | 172.5(5) | –175.1(5) | 177.2(2) | 179.57(2) | –153.4(2) |
| $C^3N^2C^{10}C^{15}$ | 20.8(3) | –16.6(2) | –7.4(6) | 3.6(8) | –3.5(4) | –0.3(4) | 27.0(2) |
| $C^3C^4C^5N^6$ | 163.3(1) | –164.3(1) | –163.6(3) | 161.7(4) | 177.2(3) | 179.6(2) | 158.6(2) |
| $C^3C^4C^9N^1$ | 1.1(2) | –1.2(2) | –0.2(4) | –1.6(5) | –1.3(3) | 0.0(3) | 5.4(2) |
| $C^3C^4C^9C^8$ | –165.3(1) | 166.4(1) | 165.8(3) | –166.9(4) | 174.7(3) | –179.2(3) | –165.7(2) |
| $C^3C^4C^{17}C^{4'}$ | –67.2(1) | 56.6(1) | 61.8(2) | –60.3(3) | – | – | – |
| $C^4C^3N^2C^{10}$ | –177.7(1) | 176.1(1) | 178.0(3) | –177.8(5) | 174.2(2) | 179.5(2) | 179.3(2) |
| $C^4C^5N^6C^7$ | –65.5(1) | 66.9(1) | 65.0(4) | –65.5(5) | –4.7(4) | 1.4(4) | –57.5(2) |
| $C^4C^5N^6C^{16}$ | 170.7(1) | –168.3(1) | –172.8(3) | 172.7(4) | –175.3(3) | –179.5(2) | 179.4(2) |
| $C^4C^{17}C^{4'}C^{5'}$ | 169.9(1) | –178.9(1) | –175.3(3) | 175.1(4) | – | – | – |
| $C^5C^4C^9N^1$ | 116.9(1) | –118.7(2) | –116.1(4) | 113.9(4) | –178.8(2) | 179.4(3) | 122.1(2) |
| $C^5C^4C^9C^8$ | –49.7(2) | 48.9(2) | 49.9(4) | –51.4(6) | –2.8(4) | 0.1(4) | –49.1(2) |
| $C^5C^4C^{17}C^{4'}$ | –175.2(3) | –178.9(1) | –175.2(3) | 175.1(4) | – | – | – |
| $C^5N^6C^7C^8$ | 63.1(2) | –63.7(2) | –63.5(4) | 63.8(6) | 23.6(4) | –3.9(6) | 60.5(2) |
| $C^7C^8C^9N^1$ | –117.6(2) | 119.8(2) | 116.1(4) | –114.3(6) | –164.6(3) | 178.4(4) | –119.1(2) |
| $C^7C^8C^9C^4$ | 47.6(2) | –46.5(2) | –48.5(5) | 49.7(6) | 20.0(4) | –2.4(5) | 50.9(2) |
| $C^8C^7N^6C^{16}$ | –173.9(1) | 171.8(1) | 175.0(4) | –174.0(5) | –165.2(2) | 176.9(4) | –177.4(2) |

**Table 3.** (Contd.)

| Angle | V1A | V1B | V2A | V2B | VIA | VIB | XIII |
|---|---|---|---|---|---|---|---|
| $C^8C^9C^4C^{17}$ | 73.3(2) | –71.9(2) | –71.3(5) | 71.7(6) | – | – | 78.1(2) |
| $C^3N^2N^1C^9$ | –6.0(2) | 7.1(2) | 4.5(4) | –3.9(5) | 1.4(3) | 0.3(3) | –5.6(2) |
| $C^9N^1N^2C^{10}$ | 177.8(1) | –176.2(1) | –177.8(3) | 176.7(4) | –175.4(2) | –179.5(2) | –176.9(2) |
| $C^9C^4C^{17}C^{4'}$ | 48.5(1) | –59.1(1) | –55.1(3) | 53.6(3) | – | – | – |

with the bridging $CH_2$ group ($C^4$–$C^{17}$ and $C^{17}$–$C^{4'}$), but the corresponding difference for polymorph **V1** molecules reaches 10° (Fig. 3, Table 3). The two independent molecules in both polymorphs are characterized by the opposite configurations of the $C^{3a}$ chiral centers ($C^{4B}$ in figures), *R*,*R* in one molecule and *S*,*S* in the other, so that crystals of both polymorphs are racemic compounds.

Differences in the conformations of fragments constituting independent molecules of the two polymorphs can be clearly demonstrated by superposition of these molecules as shown in Fig. 3 rather than by comparison of torsion angles. The two molecules of **V1** differ from each other in both pincer angle and angles of rotation of the heterocyclic fragments (Fig. 3a, Table 3), whereas the geometric structures of both molecules of **V2** are virtually similar (Fig. 3b).

The pyrazolopiperidine fragments in all molecules of both polymorphs of **V** are appreciably bent along the $C^4$–$C^9$ bond (Figs. 2, 3; Table 3) due to the presence of bridging methylene group attached to $C^{3a}$ ($C^4$ in Figs. 2, 3). This configuration considerably differs from the configuration of strongly flattened pyrazolopiperidinium cations in previously described hydrochlorides **X**–**XII** and pyrazolotetrahydropyridine **VI**, where the $C^{3a}$ atom bears no substituent [1]. As a result, the piperidine rings in **V1** and **V2** adopt a clearly defined *chair* conformation. The sum of the bonds angles at the piperidine nitrogen atoms ($N^6$) ranges within 330.0–335.6°, which corresponds to fairly high degree of their pyramidality $C_P^N$ [15] (0.61–0.74). The C=N carbon atom and pyramidal $N^6$ nitrogen atom with equatorial methyl substituent appreciably deviate from the $C^4C^5C^7C^8$ plane formed by the other atoms of the piperidine ring (Table 3). These deviations are as follows: **V1**: 0.535 ($C^{9A}$), 0.697

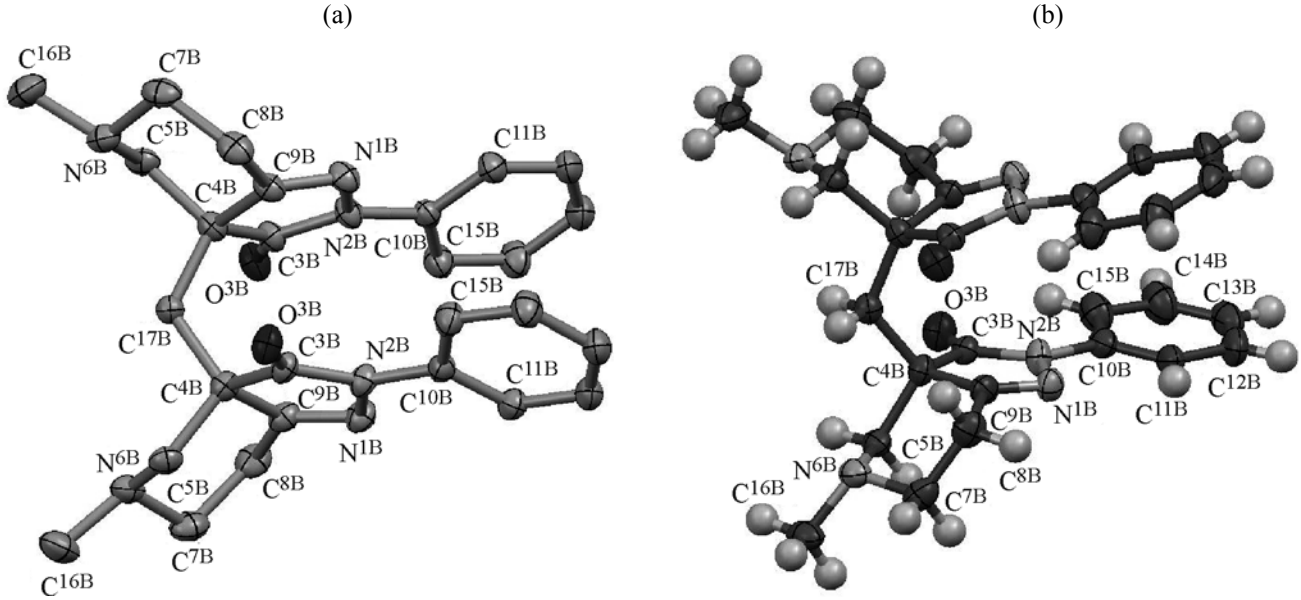


**Fig. 2.** Structures of independent molecules of dihetarylmethane polymorphs (a) **V1** and (b) **V2** according to the X-ray diffraction data. Non-hydrogen atoms are shown as thermal vibration ellipsoids with a probability of 30%. Hydrogen atoms in molecule **V1** are not shown.

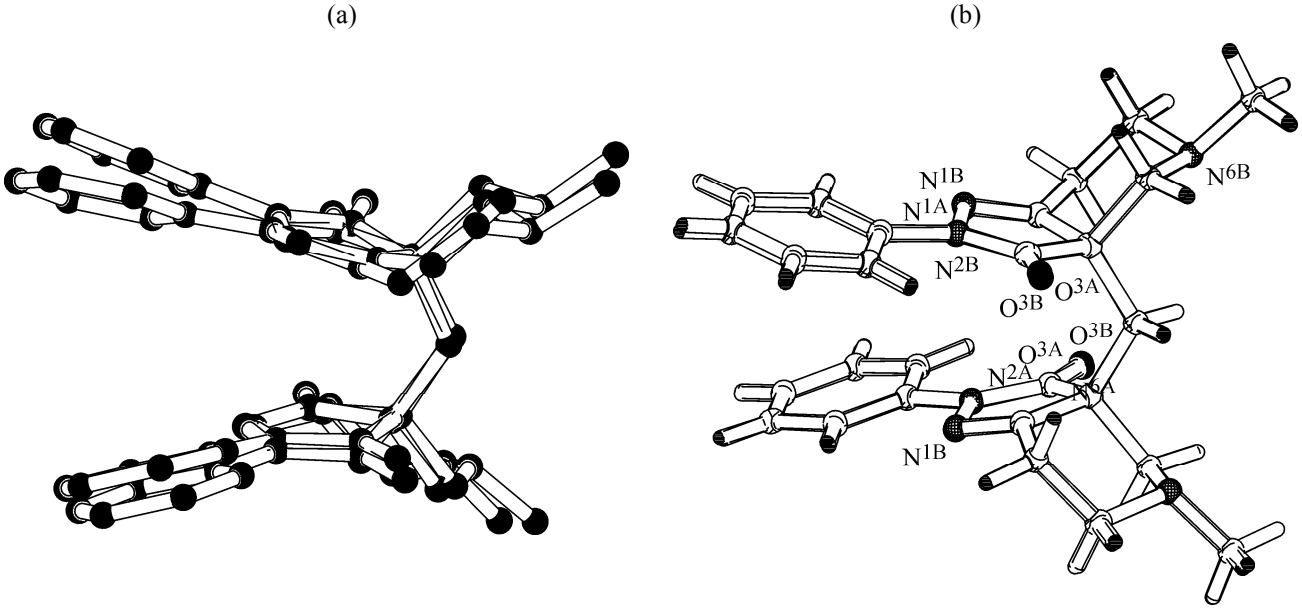


**Fig. 3.** Arbitrary superpositions of two independent molecules of dihetarylmethane polymorphs (a) **V1** and (b) **V2**. The two independent molecules of both polymorphs have opposite configurations, so that one independent molecule is superimposed onto the inverted second molecule.

($N^{6A}$), 0.522 ($C^{9B}$), 0.703 Å ($N^{6B}$); **V2**: 0.535 ($C^{9A}$), 0.702 ($N^{6A}$), 0.556 ($C^{9B}$), 0.701 Å ($N^{6B}$).

The conformation of the pyrazolone rings in all molecules **V** may be described as a weakly defined *envelope* with planar configuration of bonds at the amine nitrogen atom ($N^2$). The benzene ring attached to $N^2$ is slightly turned about the $N^2$–$C^{10}$ bond by ~15 (**V1A**), ~12.8 (**V1B**), ~6 (**V2A**), and ~3.5° (**V2B**) (Table 3). It is seen that the benzene rings in the molecules of **V1** are turned through a larger angle than in polymorph **V2** molecules. Analogous differences were also observed in the structure of the cationic parts of hydrochlorides **X**–**XII** [1].

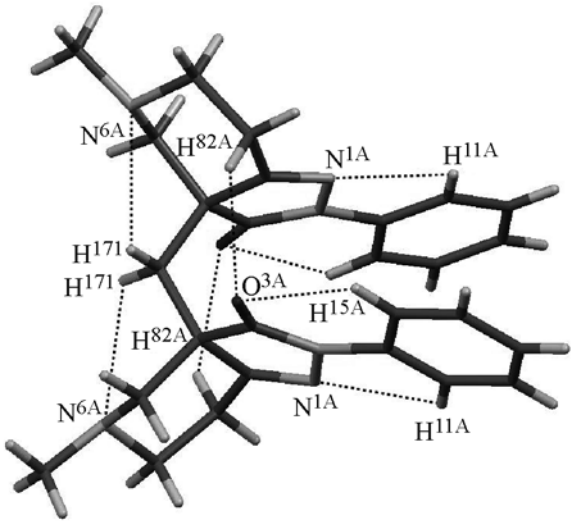


**Fig. 4.** Intramolecular hydrogen bonds system (dotted lines) in the molecules of dihetarylmethane **V** in crystal.

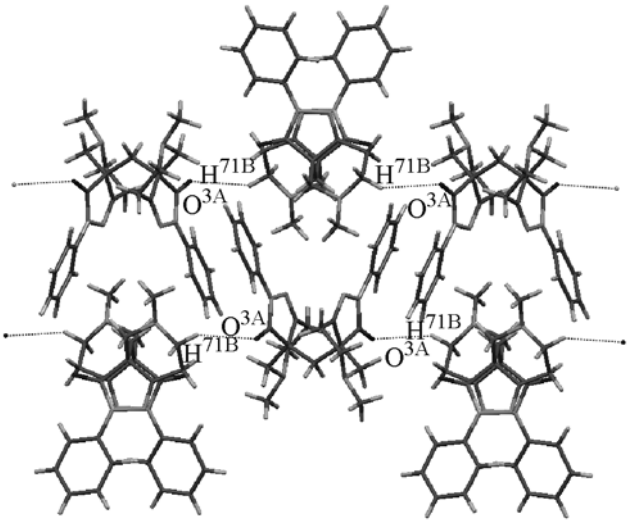


**Fig. 5.** Double chains formed by molecules of polymorph **V1** via a combination of C–H···O interactions (dotted lines) and π···π contacts. A view along the 0*b* crystallographic axis.

**Table 4.** Parameters of intra- and intermolecular contacts in the crystal structures of compounds **V–VIII**

| Comp. no. | Hydrogen bond | H···A, Å | D···A, Å | ∠DHA, deg | Comp. no. | Hydrogen bond | H···A, Å | D···A, Å | ∠DHA, deg |
|---|---|---|---|---|---|---|---|---|---|
| **V1** | $C^{8A}H^{81A}\cdots O^{3A}$ | 2.49 | 3.320(3) | 143 | **VI** | $C^{11A}–H^{11A}\cdots N^{1A}$ | 2.44 | 2.773(3) | 101 |
| | $C^{8B}–H^{82B}\cdots O^{3B}$ | 2.59 | 3.274(3) | 128 | | $C^{11B}–H^{11B}\cdots N^{1B}$ | 2.42 | 2.768(4) | 102 |
| | $C^{11A}–H^{11A}\cdots N^{1A}$ | 2.48 | 2.804(2) | 101 | | $C^{15A}–H^{15A}\cdots O^{3A}$ | 2.24 | 2.882(3) | 126 |
| | $C^{11B}–H^{11B}\cdots N^{1B}$ | 2.45 | 2.789(2) | 102 | | $C^{15B}–H^{15B}\cdots O^{3B}$ | 2.27 | 2.905(3) | 125 |
| | $C^{15A}–H^{15A}\cdots O^{3A}$ | 2.39 | 2.957(3) | 119 | | $C^{5A}–H^{5A}\cdots O^{3B\,d}$ | 2.38 | 3.217(3) | 150 |
| | $C^{15B}–H^{15B}\cdots O^{3B}$ | 2.37 | 2.950(2) | 120 | | $C^{16A}–H^{161A}\cdots O^{3B\,d}$ | 2.59 | 3.405(4) | 143 |
| | $C^{17B}–H^{173B}\cdots N^{6B}$ | 2.62 | 3.007(2) | 104 | | $C^{14B}–H^{14B}\cdots O^{3A\,e}$ | 2.47 | 3.184(4) | 134 |
| | $C^{17A}–H^{171A}\cdots N^{6A}$ | 2.63 | 3.049(2) | 106 | **VII** | $N^{2}–H^{2}\cdots O^{3}$ | 2.19 | 3.054(2) | 167 |
| | $C^{7B}–H^{71B}\cdots O^{3A\,a}$ | 2.67 | 3.498(3) | 123 | **VIII** | $C^{11}–H^{11}\cdots N^{1}$ | 2.49 | 2.813(3) | 100 |
| **V2** | $C^{8B}–H^{81B}\cdots O^{3B}$ | 2.44 | 3.200(7) | 134 | | $C^{15}–H^{15}\cdots O^{3}$ | 2.40 | 2.953(3) | 117 |
| | $C^{8A}–H^{82A}\cdots O^{3A}$ | 2.48 | 3.232(5) | 134 | | $N^{6}–H^{6}\cdots Cl^{1}$ | 2.04(3) | 3.037(2) | 153(3) |
| | $C^{11A}–H^{11A}\cdots N^{1A}$ | 2.43 | 2.785(6) | 103 | | $O^{11}–H^{111}\cdots Cl^{1}$ | 2.08(3) | 3.139(2) | 171(3) |
| | $C^{14A}–H^{14A}\cdots O^{3B}$ | 2.70 | 3.526(9) | 149 | | $O^{11}–H^{112}\cdots O^{3\,f}$ | 1.96(2) | 2.933(3) | 175(3) |
| | $C^{15A}–H^{15A}\cdots O^{3A}$ | 2.30 | 2.923(6) | 124 | | $C^{5}–H^{51}\cdots Cl^{1\,f}$ | 2.71 | 3.633(2) | 156 |
| | $C^{11B}–H^{11B}\cdots N^{1B}$ | 2.37 | 2.736(7) | 103 | | $C^{7}–H^{71}\cdots O^{11\,g}$ | 2.49 | 3.305(3) | 140 |
| | $C^{15B}–H^{15B}\cdots O^{3B}$ | 2.31 | 2.920(6) | 123 | | $C^{16}–H^{161}\cdots O^{3\,h}$ | 2.56 | 3.462(3) | 153 |
| | $C^{17B}–H^{173B}\cdots N^{6B}$ | 2.65 | 3.045(4) | 105 | | | | | |
| | $C^{17A}–H^{171A}\cdots N^{6A}$ | 2.66 | 3.046(4) | 104 | | | | | |
| | $C^{7A}–H^{71A}\cdots O^{3A\,b}$ | 2.55 | 3.512(5) | 174 | | | | | |
| | $C^{16A}–H^{161}\cdots O^{3B\,c}$ | 2.70 | 3.440(6) | 135 | | | | | |

[a] Symmetry operations: $x$, $1 – y$, $1/2 + z$. [b] $3/2 – x$, $–1/2 + y$, $1 – z$. [c] $1/2 + x$, $1/2 – y$, $1 – z$. [d] $–x$, $1/2 + y$, $1/2 – z$. [e] $–x$, $–1/2 + y$, $1/2 – z$. [f] $1 – x$, $2 – y$, $1 – z$. [g] $1 – x$, $–1/2 + y$, $3/2 – z$. [h] $1 – x$, $1/2 + y$, $3/2 – z$.

Intra- and intermolecular interactions in both polymorphs of **V** include mainly hydrogen bonds like C–H···N and C–H···O (Table 4), as well as intramolecular π···π contacts between the five-membered rings (Table 5). Taking into account structural similarity of molecules **VA** and **VB**, it should be emphasized that the modes of intramolecular hydrogen bonding are identical for in all molecules of **V** (Fig. 4) with an accuracy of 1/2 molecule (independent part).

As seen from the data in Table 5, π···π contacts with similar parameters exist between the five-membered rings in molecules of both polymorphs. Presumably, these contacts provide additional stabilization of the pincer conformation. The distances between the centroids of the phenyl rings are much longer, and they are considerably different in molecules **A** and **B** of polymorphs **V1** and **V2**: 5.112(3) and 6.563(2) Å in **V1A** and **V1B** and 5.964(4) and 5.643(4) Å in **V2A** and **V2B**, respectively.

The supramolecular structure of polymorph **V1** is determined by a combination of three types of intermolecular interactions. Hydrogen bonds C–H···O involving the $O^{3A}$ carbonyl oxygen atom of **V1A** give rise to chains consisting of alternating molecules **A** and **B** along the 0*c* crystallographic axis (Table 4). Two neighboring chains are linked to each other through π···π contacts between the aromatic substituents with an intercentroid distance of 4.837(3) Å, dihedral angle of 0°, and shortest interplanar distance of 3.29 Å (Fig. 5).

**Table 5.** Parameters of π···π and CH···π contacts involving the five-membered rings in the crystal structures of compounds **V**, **VII**, and **XIII** [30][a]

| Compound no. | Contact | $d_1$ | $d_2$ | α | β |
|---|---|---|---|---|---|
| **V1A** | Cg···Cg' | 3.128(2) | 3.063 | 18.42 | 11.76 |
| **V1B** | Cg···Cg' | 3.081(2) | 3.032 | 16.75 | 10.21 |
| **V2A** | Cg···Cg' | 3.083(2) | 3.038 | 19.75 | 9.90 |
| **V2B** | Cg···Cg' | 3.133(3) | 3.072 | 22.55 | 11.30 |
| **VII** | Cg···Cg [b] | 5.279(2) | 3.21 | 0.0 | 52.5 |
| | $C^3$–$H^{31}$···Cg2 [c] | 2.86 | – | 140 | – |
| | $C^1$–$H^{103}$···Cg2 [d] | 2.84 | – | 158 | – |
| **XIII** | $C^3$–$H^{31}$···Cg [e] | 2.86 | – | 140 | – |
| | $C^1$–$H^{103}$···Cg [f] | 2.84 | – | 158 | – |

[a] $d_1$ is the distance between the centroids of rings (Cg), Å; $d_2$ is the shortest distance between the ring planes, Å; α is the dihedral angle between the ring planes, deg; and β is the ring overlap angle, deg. Symmetry operations: [b] $1 - x, -y, -z$. [c] $x, 1/2 - y, 1/2 + z$. [d] $-x, -y, 1 - z$. [e] $x, 1/2 - y, 1/2 + z$. [f] $-x, -y, 1 - z$.

The third type of interactions is responsible for binding of similar neighboring double chains. This interaction comprises exclusively "jamming" of bridging methylene groups between two phenyl substituents of molecules belonging to neighboring double chains. It may be clearly illustrated by two projections of crystal packing of polymorph **V1** shown in Fig. 6. As a result, a layer is formed from the parallel double chains in the *a*0*c* plane (Fig. 6). On the whole, the crystal packing of **V1** may be represented as parallel laying of similar laminar structures shown in Fig. 6 along the 0*b* crystallographic axis. Interactions between such layers involve only conventional van der Waals contacts. Despite relatively low crystal packing factor (65.8%), unit cells possess no voids capable of accommodating solvent molecules.

No intermolecular π···π contacts is observed in rhombic polymorph **V2**, and intermolecular interactions are represented mainly by pair C–H···O hydrogen bonds. The two independent molecules of **V2**, being conformationally identical (with opposite configurations of the chiral atom; Fig. 3), have different molecular environments and are involved in different interactions. The supramolecular structure of **V2** is characterized by formation of **V2A**···**V2B** head-to-head hydrogen-bonded dimers (Fig. 7). These dimers are formed with participation of only $O^{3B}$ carbonyl oxygen atoms of molecules **V2B**, whereas the $O^{3A}$ atoms in molecules **V2A** link the H-dimers with each other to produce a zigzag band with outer hydrophobic margins composed of phenyl substituents (Fig. 8a). The $O^{3B}$ atoms are also involved in bifurcated hydrogen bonds which combine similar bands with formation of a two-dimensional system, a corrugated bilayer consisting of H-bonded molecules, which is parallel to the *a*0*b* crystallographic plane and bounded at the outer sides by phenyl substituents (Table 5). The reason is that molecules **A** and **B** in the H-dimer are turned relative to each other through an angle of 90°, and the two terminal hydrogen bonds appear mutually orthogonal (Fig. 8b).

The outer sides of the H-bonded bilayer (Fig. 8) are composed of molecules **V2B** that are (*R*,*R*)-stereoisomers. The inner part consists of (*S*,*S*)-isomeric molecules **V2A**, i.e., both enantiomers in crystal are spatially separated. This suggests to some extent the ability of racemic compound **V2** to undergo spontaneous resolution. Further development of the crystal packing of **V2** involves exclusively π···π (like T-stacking) and C–H···π contacts between molecules **B** belonging to neighboring bilayers, so that the corrugated bilayers are linked along the 0*c* crystallographic axis. Here, the C–H···O interactions are observed only with outer molecules **V2B** within a corrugated bilayer. However, the calculated packing factor (64.3%) turned out to be even lower than those typical of crystalline organic compounds (65–75%) [16].

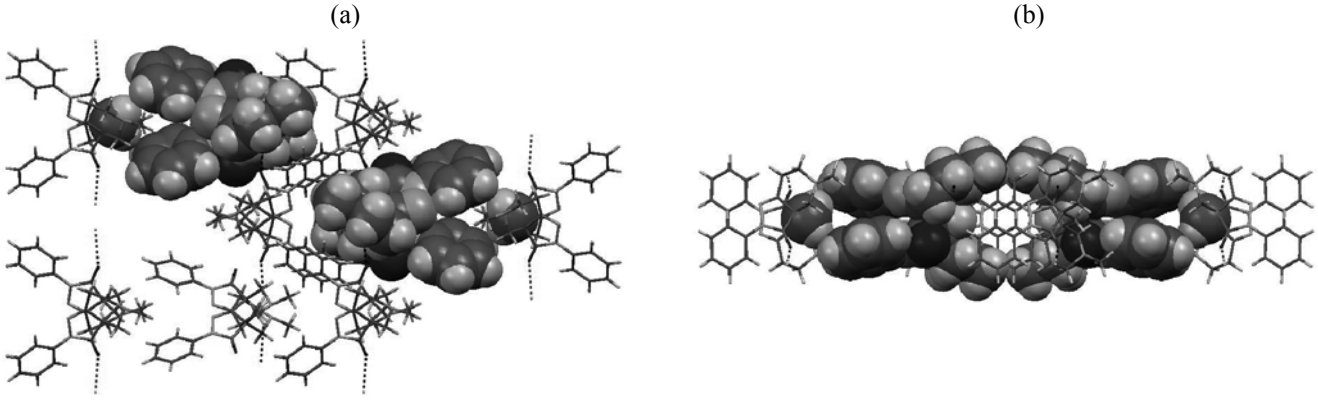


**Fig. 6.** Projections along the (a) 0*a* and (b) 0*c* axes of crystal packing of polymorph **V1**. Hydrogen bonds are shown with dotted lines; methylene groups in molecules belonging to neighboring bilayers are also shown as van der Waals spheres.

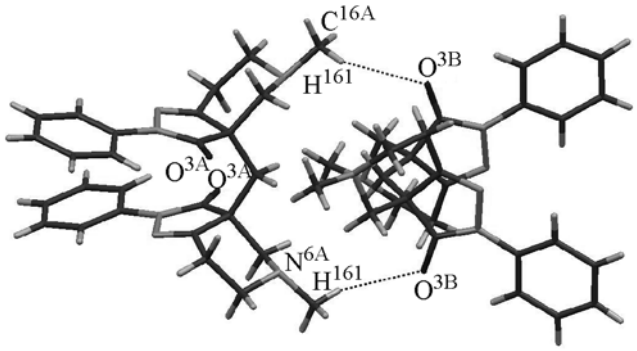


**Fig. 7.** Hydrogen-bonded dimer formed by molecules **A** and **B** of rhombic polymorph **V2**. Hydrogen bonds are shown with dotted lines.

Pyrazolotetrahydropyridine **VI** was initially isolated by chromatography from the complex mixture of products obtained in the reaction of phenylhydrazine with keto ester **Ia** with a view to synthesize pyrazolopiperidine **IIa** [3]. The structure of **VI** was assigned on the basis of spectral data. Unlike compound **V**, the $^1$H NMR spectrum of **VI** in $CDCl_3$ contained a singlet at δ 7.71 s (1H, 4-H), and the intensity of the $CH_2$ signals was lower. Compound **VI** displayed in the IR spectrum absorption bands due to stretching vibrations of aromatic C=C bonds (1593 $cm^{-1}$), carbonyl absorption band at 1663 $cm^{-1}$ (which was displaced to lower frequencies due to conjugation), and a very strong band at 1626 $cm^{-1}$, which is likely to originate from stretching vibrations of the conjugated bond system in the heterocyclic fragment. This assumption is confirmed by a good agreement between the experimental and calculated $^{15}$N and $^{13}$C chemical shifts in the NMR spectra of **VI** (an example of such correlation for carbon chemical shifts is shown in Fig. 9; $R^2 = 0.999$).

The structure of compound **VI** in crystal was also determined by X-ray analysis (Fig. 10); single crystals were obtained by crystallization from acetone. Like compound **V**, the independent part of the unit cell of **VI** contains two molecules **VIA** and **VIB**. The geometric parameters are given in Tables 1–3, and the molecular structures are shown in Fig. 10. Figure 11 shows an arbitrary superposition of two independent molecules **VIA** and **VIB**, which reveals different conformations of the tetrahydropyridine fragments therein and some difference in the rotation of the phenyl substituent with respect to the five-membered ring plane.

The $C^5$–$N^6$ bonds in the tetrahydropyridine rings of **VIA** and **VIB** (1.312–1.315 Å) are appreciably shorter than the other C–$N^6$ bonds (1.446–1.464 Å), which was not observed in polymorphs **V1** and **V2**. Despite the presence of contiguous $C^4$=$C^5$ double bond and shortening of the neighboring $C^3$–$C^4$ bond to ~1.430 Å, the $C^3$=$O^3$ carbonyl bond length in both molecules of

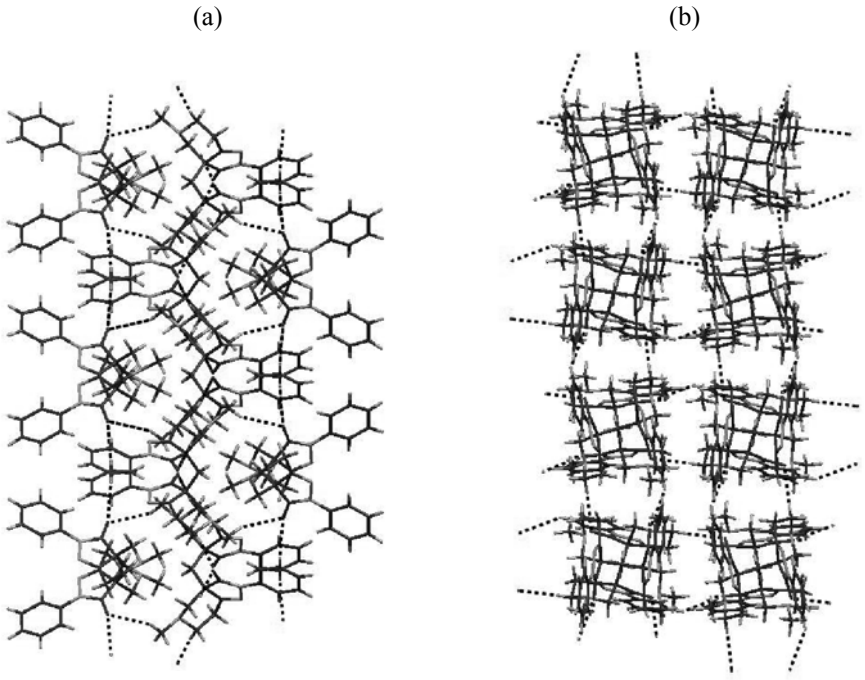


**Fig. 8.** Projections along the (a) 0*b* and (b) 0*c* axes of a corrugated bilayer formed by hydrogen-bonded molecules of polymorph **V2** (C–H···O hydrogen bonds are shown with dotted lines).

**VI** is the same as in all molecules of **V** (Table 1). It should be noted that, despite similarity of the $C^7$–$N^6$ bond lengths in molecules of both compounds, the $C^7$–$C^8$ bonds in **VI** are slightly shorter and different in independent molecules **VIA** and **VIB** [1.483(5) and 1.401(4) Å, respectively].

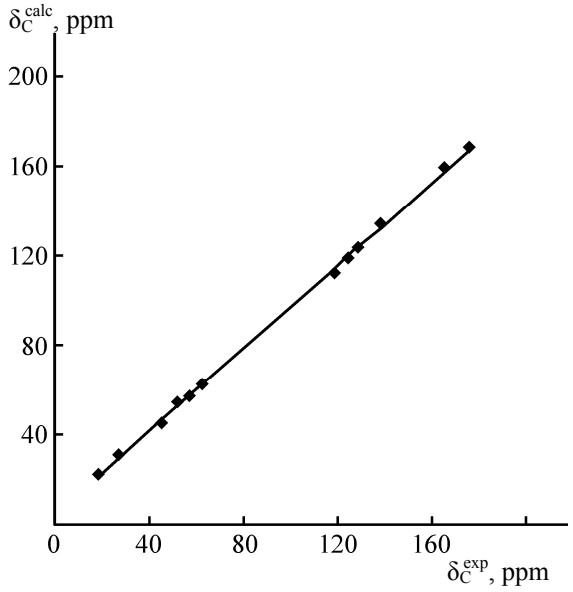


**Fig. 9.** Correlation of the experimental ($CDCl_3$) and calculated $^{13}C$ chemical shifts of pyrazolotetrahydropyridine **VI**.

The presence of a $C^4$=$C^5$–$N^6$ enamine bond system makes the tetrahydropyridine ring in **VI** flattened (Table 3, Fig. 11); as a result, the entire pyrazolopyridine fragment becomes flatter: the dihedral angle between the five-membered ring and the $C^9C^4C^5N^6C^7$ fragment is as small as ~5°. The configuration of bonds on the amino nitrogen atom ($N^6$) is planar due to conjugation in the enamine fragment (the sum of the bond angles on the $N^6$ nitrogen atom approaches 360°, Table 2).

The benzene rings in **VIA** and **VIB** are turned about the $N^2$–$C^{10}$ bond through a smaller angle (~3.5 and 0.5°, respectively) than in polymorph **V1**, and these angles are close to those found for **V2A** and **V2B** (Table 3). This leads to strengthening of the intramolecular hydrogen bonds $C^{15}$–$N^{15}\cdots O^3$ and $C^{11}$–$H^{11}\cdots N^1$ and hence shortening of the $C^{15}\cdots O^3$ and $C^{11}\cdots N^1$ distances and increase of the $C^{15}N^{15}O^3$ and $C^{11}H^{11}N^1$ angles (Table 4).

The supramolecular structure of compound **VI** in crystal is also determined by only C–H···O and C–H···N hydrogen bonds, while classical hydrogen bonds are lacking. The C–H···O bonds link molecules

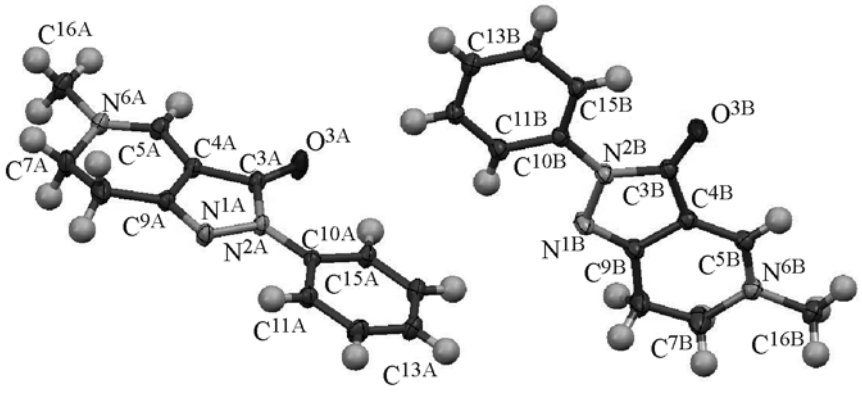


**Fig. 10.** Structures of independent pyrazolotetrahydropyridine molecules **VIA** and **VIB** according to the X-ray diffraction data. Non-hydrogen atoms are shown as thermal vibration ellipsoids with a probability of 50%, and hydrogen atoms are shown as spheres with an arbitrary radius.

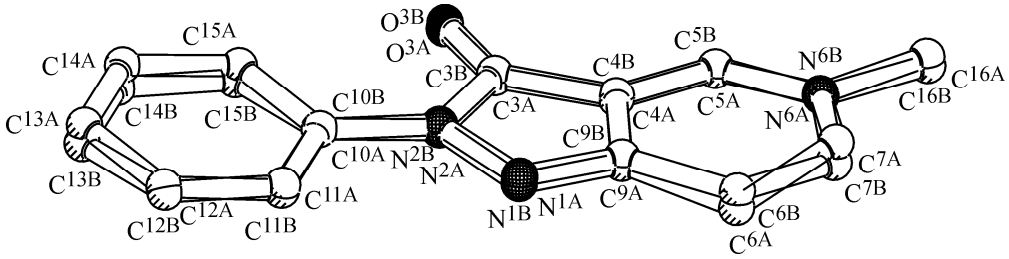


**Fig. 11.** Arbitrary superposition of two independent pyrazolotetrahydropyridine molecules **VIA** and **VIB**.

**VIA** and **VIB** to dimers, and the C–H···N bonds give rise to H-tetramer (Fig. 12a). The H-dimers are linked to the H-tetramer only through the $N^2$ atom of one independent molecule (**VIA**). We believe that such H-tetramer formed by a combination of C–H···O and C–H···N hydrogen bonds should be regarded as a supramolecular synthon. The H-tetramers are linked to each other via bifurcated hydrogen bond involving the $O^{3A}$ atom to produce skewed stacks of molecules arranged antiparallel to each other (Fig. 12b).

We succeeded in isolating a small amount of pure hydrazonopyrrolidine **VII** together with compounds **V** and **VI** by treatment of sesquihydrochloride **X** with potassium carbonate in methanol. Hydrazone **VII** in crystal and in solution (DMSO-$d_6$) exists as a single *E* isomer (Fig. 13), while in $CDCl_3$ a mixture of approximately equal amounts of the *Z* and *E* isomers is formed. Presumably, the *E*/*Z* isomerization is promoted by $CDCl_3$. 1-Methyl-3-(2-phenylhydrazinylidene)pyrrolidin-2-one (**VII**) was synthesized previously by reaction of benzenediazonium salt with 2-chloro-1-methyldihydropyrrolium chloride [17]. Although the properties of compound **VII** isolated by us coincided with published data [17], we determined its molecular geometry in crystal by X-ray analysis. The independent part of a unit cell of **VII** includes one molecule whose structure is shown in Fig. 13, and the crystal packing, in Fig. 14. The bond lengths and bond angles in the benzene ring and hydrazone fragment are typical of phenyl groups with an electron-donating substituent, such as phenylhydrazones [13, 14].

Molecules **VII** in crystal are linked through N–H···O hydrogen bonds to form a flat band along the 0*a* crystallographic axis (Fig. 14a, Table 4). The H-bonded bands are packed parallel to the *a*0*c* crystallographic plane (Fig. 14b) via a combination of C–H···π and π···π contacts between the bands (Table 5). Such arrangement of molecules in crystal ensures their tight packing (the calculated packing factor is 70.7%). Even tighter packing and formation of additional π···π contacts are hampered by the methylene and methyl groups which appear just under the aromatic fragments of neighboring molecules thus preventing them from approaching each other to a shorter distance. This parallel packing of molecules **VII** in crystal leads to considerable anisometry of the

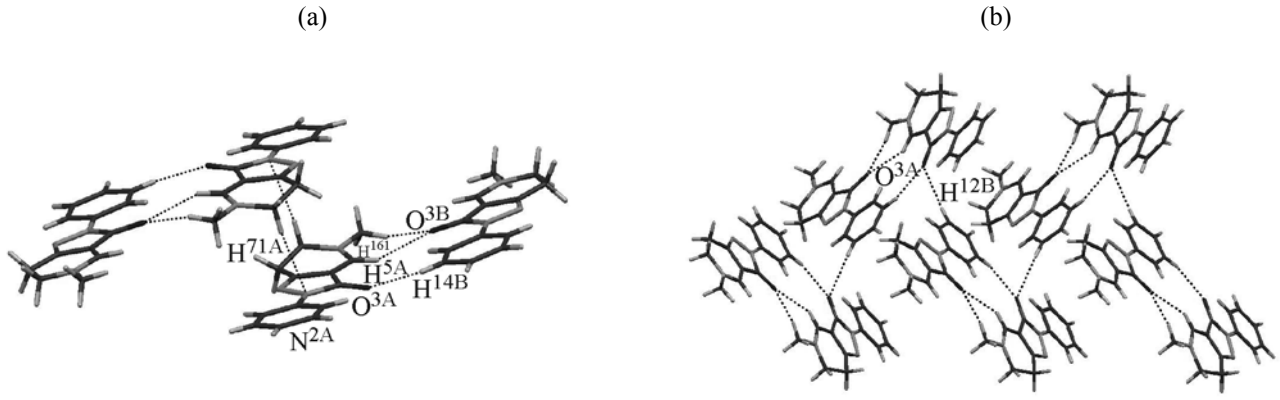


**Fig. 12.** (a) Structure of the hydrogen-bonded tetramer formed by pyrazolotetrahydropyridine molecules **VIA** and **VIB** and (b) its crystal packing; hydrogen bonds are shown with dotted lines.

crystal structure, and it may be responsible for anisotropic properties of crystalline compound **VII**.

Depending on the conditions of synthesis of pyrazolopiperidine **IIa**, purification method, or solvent nature, the composition of its transformation products strongly varies. For example, dissolution of **IIa** in DMSO leads to formation of pyrazolotetrahydropyridine **VI** in a very high yield. The reaction of phenylhydrazine with keto esters **I** (R = Me, Et) in boiling alcohols or benzene gives mainly compounds **V**–**VII**. When pyrazolopiperidine **IIa** prepared at 15–20°C was heated in boiling methanol for 4 h, we isolated compounds **V** and **VI** and a yellow oily substance. According to the $^{1}$H, $^{13}$C, and $^{15}$N NMR data, the latter contained approximately equal amounts of 3a,5-dimethyl-2-phenyl-3,3a,4,5,6,7-hexahydro-2*H*-pyrazolo[4,3-*c*]pyridin-3-one (**VIII**) and methyl 3-(2-phenylhydrazinylidene)-4,5-dihydro-3*H*-pyrrole-2-carboxylate (**IX**).

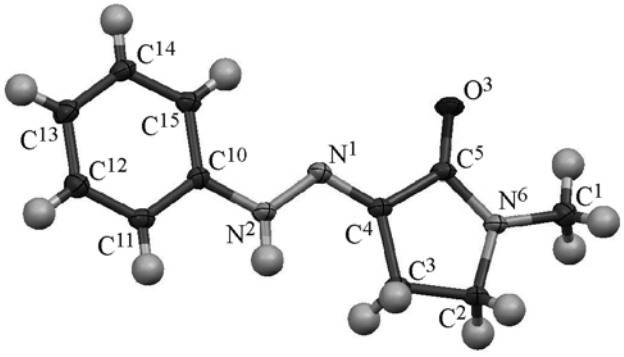


**Fig. 13.** Structure of the molecule of phenylhydrazonopyrrolidine **VII** in crystal according to the X-ray diffraction data. Non-hydrogen atoms are shown as thermal vibration ellipsoids with a probability of 50%, and hydrogen atoms are shown as spheres with an arbitrary radius. Selected geometric parameters (bond lengths and bond and torsion angles): $N^1$–$C^4$ 1.285(3), $N^1$–$N^2$ 1.356(3), $N^2$–$H^2$ 0.88(3), $N^2$–$C^{10}$ 1.380(3), $O^3$–$C^5$ 1.233(3), $C^4$–$C^5$ 1.477(4), $C^5$–$N^6$ 1.349(3) Å; $N^2N^1C^4$ 116.6(2)°, $N^1N^2C^{10}$ 119.9(2)°, $N^1N^2H^2$ 122(1)°, $O^3C^5N^6$ 125.1(2)°, $O^3C^5C^4$ 128.4(2)°, $N^1C^4C^5$ 121.3(2)°, $N^1C^4C^3$ 129.0(2)°, $N^2C^{10}C^{11}$ 119.0(2)°, $C^5N^6C^1$ 125.6(2)°, $C^1N^6C^2$ 119.4(2)°; $C^4N^1N^2C^{10}$ 177.6(2)°, $N^1C^4C^5O^3$ 3.1(4)°, $N^1N^2C^{10}C^{11}$ 179.6(2)°.

We failed to separate oily mixture **VIII**/**IX** into individual components, and their structure was analyzed by NMR spectroscopy of their mixture. Signals of particular compounds **VIII** and **IX** in the $^{1}$H NMR spectra ($CDCl_3$) were identified using the DOSY technique due to appreciable difference in their self-diffusion coefficients, $1.32\times10^{-9}$ and $1.06\times10^{-9}$ m$^2$/s, respectively. Their structure was determined with the aid of various homo- and heteronuclear shift correlation techniques (COSY, $^{1}$H–$^{13}$C/$^{1}$H–$^{15}$N HSQC and HMBC). The assignment made was additionally confirmed by a good agreement between the calculated (DFT GIAO) and experimental $^{13}$C and $^{15}$N chemical shifts; the correlation for compound **VIII** is given in Fig. 15 ($R^2 = 0.999$).

Apart from structure assignment, the NMR data allowed us to refine isomer compositions of phenylhydrazones **VII** and **IX** in solution. According to the NOE data and the calculated and experimental $^{13}$C and $^{15}$N chemical shifts, phenylhydrazone **VII** in DMSO-$d_6$ exists exclusively as *E* isomer, whereas in $CDCl_3$ a mixture of *E* and *Z* isomers is formed, the *E* isomer prevailing (Fig. 16). By contrast, the NOE observed between the NH and 4-H protons led us to conclude that phenylhydrazone **IX** in DMSO-$d_6$ and $CDCl_3$ has solely *E* configuration (Scheme 4).

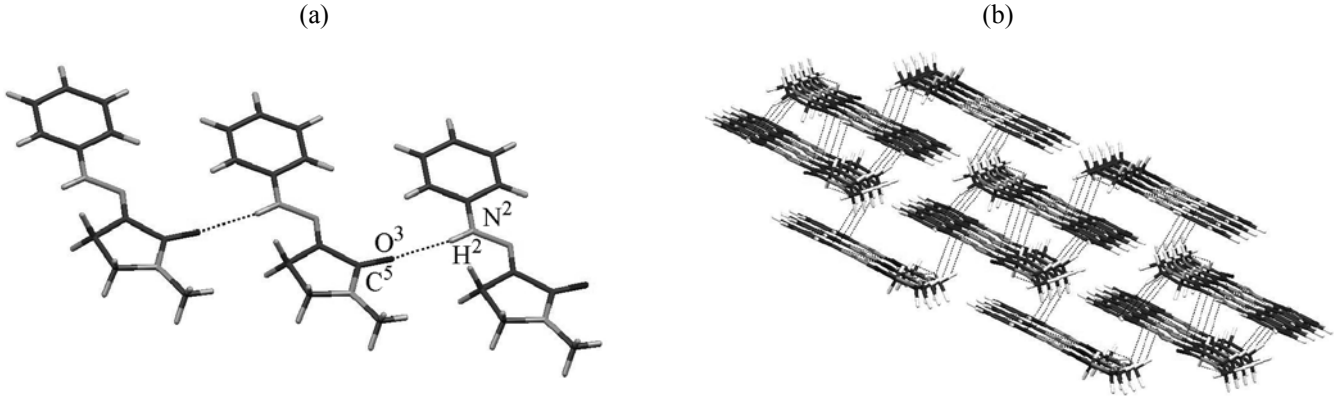


**Fig. 14.** (a) Intermolecular hydrogen bonds and (b) crystal packing of hydrazone **VII**; C–H···π and π···π contacts and N–H···O hydrogen bonds are shown with dotted lines. Views along the (a) 0*b* and (b) 0*a* crystallographic axes.

3a-Methyl derivative **VIII** forms stable hydrochloride **XIII** which was isolated as monohydrate. Its structure was determined by X-ray analysis. Hydrochloride **VIII**·HCl·$H_2O$ crystallizes in monoclinic crystal system (space group $P2_1/c$) with one independent molecule in the asymmetric part of the unit cell. The structure of hydrochloride **XIII** is shown in Fig. 17, its geometric parameters are given in Tables 1–3, and intramolecular hydrogen bonds and intermolecular contacts are presented in Tables 4 and 5.

The conformation of the pyrazolopiperidine fragment in the cationic part of **XIII** is the same as in molecules **V**. It is bent along the $C^4$–$C^9$ bond (Fig. 17; Tables 2, 3). The bond angles and bond angles therein are closer to those found for polymorphs **V1** and **V2** than to the corresponding values for tetrahydropyridine molecule **VI**. Only the bonds formed by the $N^6$ atom with carbons are longer than those in **V** and **VI** (Table 1).

As in molecules **V** and **VI**, the benzene ring in the cation of **XIII** is turned about the $N^2$–$C^{10}$ bond with respect to the pyrazolone ring plane through an angle of ~16.5° which is slightly larger than the corresponding angle in molecules **V1** (Table 3). Despite acoplanarity of the benzene and pyrazolone rings in **XIII**, there exist hydrogen bonds $C^{15}$–$H^{15}$···$O^3$ and $C^{11}$–$H^{11}$···$N^1$ (Table 4), as was observed in the molecules of **V**, **VI** (Table 4), and hydrochlorides **X**–**XII** [1].

Analysis of intermolecular interactions in the crystal structure of hydrochloride **XIII** revealed the presence of various hydrogen bonds, as well as of C–H···π contacts (Tables 4, 5). Conventional O–H···O hydrogen bonds involving the $O^3$ carbonyl oxygen atom hold together the hydration water molecule and the cation of **XIII**. The chloride ion in turn is linked to both the cation through the $N^6$–H···Cl bond and with the water molecule through the O–H···Cl bond. A combination of the above interactions leads to the formation of pseudo-hexamers consisting of two protonated molecules **VIII**, two water molecules, and two chloride ions (Fig. 18).

The $O^{11}$ oxygen atom (water molecule) also participates in bifurcated C–H···O hydrogen bonds with $H^{71}$ and $H^{52}$ in the piperidine methylene groups. Analogous hydrogen bonds are also observed between the methyl hydrogen ($H^{161}$) and $O^3$ carbonyl oxygen atom and between $H^{14}$ in the benzene ring and $O^3$ of the symmetry-related molecule. The C–H···Cl

**Scheme 4.**

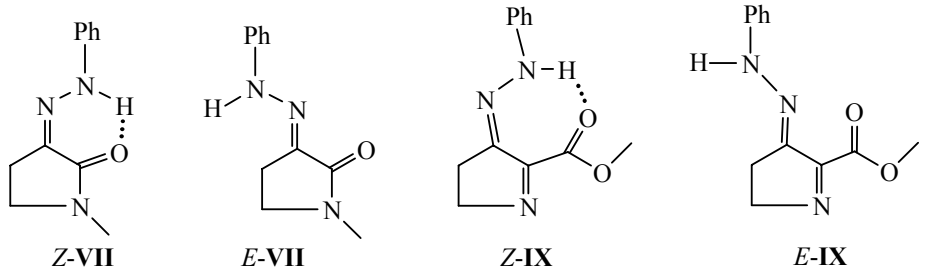


*Z*-**VII** *E*-**VII** *Z*-**IX** *E*-**IX**

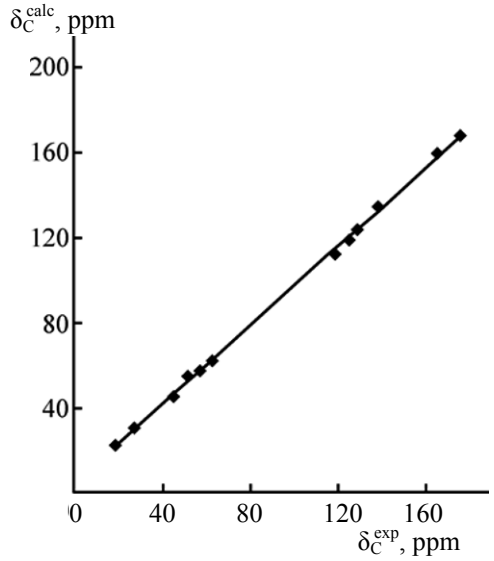


**Fig. 15.** Correlation between the experimental ($CDCl_3$) and calculated $^{13}C$ chemical shifts of compound **VIII**.

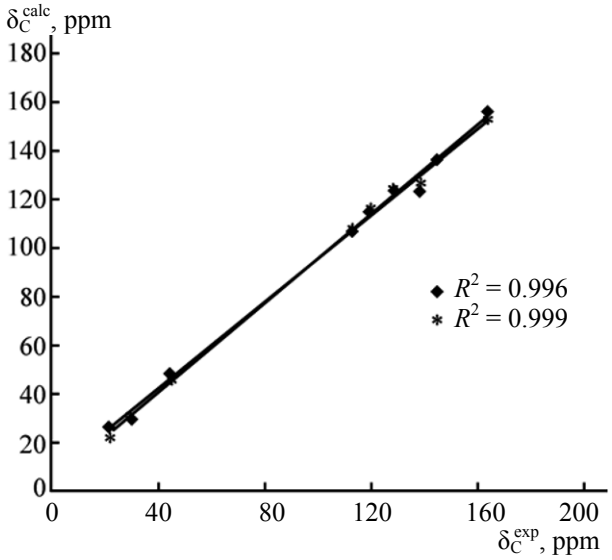


**Fig. 16.** Correlation between the experimental ($CDCl_3$) and calculated $^{13}C$ chemical shifts of the *E* (rhombs) and *Z* isomers (asterisks) of phenylhydrazone **VII**.

hydrogen bonds with $Cl^1$ involve $H^{51}$ of the piperidine ring and $H^{163}$ and $H^{171}$ methyl hydrogens. These C–H···O and C–H···Cl hydrogen bonds link pseudo-hexamers of **XIII** to produce three-dimensional network (Fig. 19) with water molecules and chloride ions located in the pseudochannels, though there is no direct contact between water molecules or chloride ions in the channels.

The three-dimensional network (Fig. 19) is additionally stabilized by C–H···π contacts between $C^8H^{81}$ and benzene ring: the shortest distance from the $H^{81}$ hydrogen atom and the corresponding centroid is 2.80 Å, and the dihedral angle is 127°. No π···π contacts were observed in the crystal structure of hydrochloride **XIII**, presumably due to steric hindrances originating from the conformation of the bicyclic system. Despite unfavorable conformations of the heterocyclic fragment and the whole molecule, the presence of anions and hydration water molecules ensures a fairly high packing factor (71.8%) due to the absence of additional voids potentially accessible to solvent molecules.

It is difficult to unambiguously interpret pathways of the transformation of pyrazolopiperidine **IIa** into compounds **V**–**IX**. Presumably, these reactions involve one-step, consecutive, and interrelated processes. The former assumption [3, 5] according to which pyrazolo-tetrahydropyridine **VI** is formed via autooxidation of pyrazolopiperidine **IIa** was confirmed experimentally. In a few hours after dissolution, the $^1H$ and $^{13}C$ NMR spectra of **IIa** in DMSO-$d_6$ contained signals typical of pyrazolotetrahydropyridine **VI**. After two days, the fraction of **VI** in solution attained ~85%. Oxidation processes also occurred in solutions of **IIa** in nonpolar solvents (PhH, $CHCl_3$, $CH_2Cl_2$, etc.) on storage, but different reactions clearly dominated.

We presumed in [3] that dihetarylmethane (**V**) is formed from pyrazolopiperidine **IIa** and formaldehyde which can be generated in the reaction mixture from methanol. The latter was used as solvent or it may

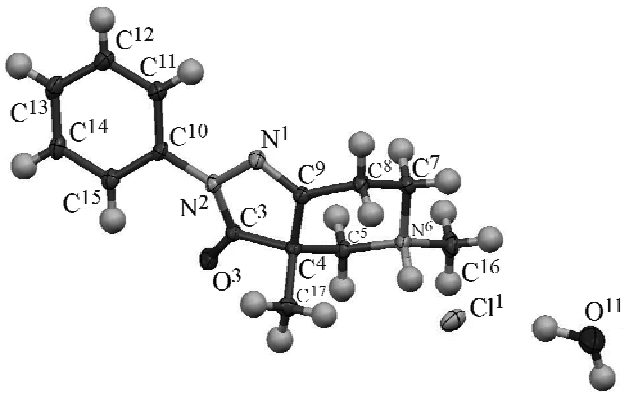


**Fig. 17.** Structure of the molecule of hydrated hydrochloride **XIII** (**VIII**·HCl·$H_2O$) in crystal according to the X-ray diffraction data. Non-hydrogen atoms are shown as thermal vibration ellipsoids with a probability of 50%, and hydrogen atoms are shown as spheres with an arbitrary radius.

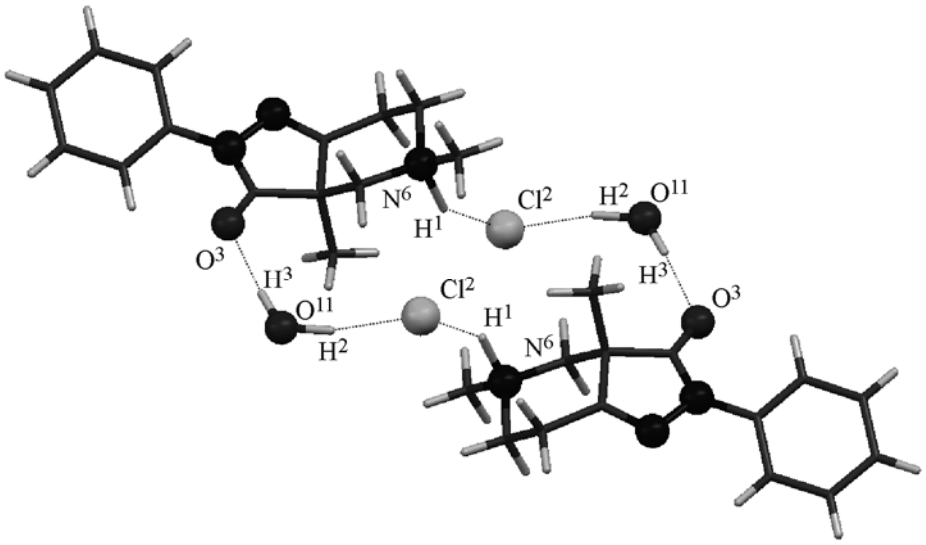


**Fig. 18.** Pseudohexamers formed in the crystal structure of hydrochloride hydrate **XIII** via hydrogen bonds (dotted lines) with water molecules.

originate from the methoxycarbonyl fragment of the initial keto ester (**Ia**, R = Me). In fact, addition of formaldehyde to the reaction mixture and even to the mother liquors increases the yield of **V**. However, the reaction with keto ester **Ib** (R = Et) in both methanol and ethanol gave the same product rather than the corresponding 1,1-dihetarylethane derivative. Later, we detected compound **VIII** among the transformation products of **IIa** in boiling methanol and presumed possible addition of **VIII** to the double bond of pyrazolotetrahydropyridine **VI** with formation of dihetarylmethane **V**. However, this assumption has not been proved so far. After heating of a mixture of pyrazolotetrahydropyridine **VI** and mixture **VIII**/**IX** in methanol, no dihetarylmethane **V** was detected by TLC, though initial compound **VI** was also absent in the reaction mixture.

Analysis of published data revealed the ability of piperidine [18, 19], 4-oxopiperidine [20], and 4-iminopiperidine derivatives, including those fused to aza cycles [21, 22], to undergo various transformations such as ring contraction reactions. These transformations may involve formation of carbonyl compounds in which the carbonyl carbon atom was formerly a part of the piperidine ring [20]. The presence of a quaternary nitrogen atom strongly facilitates such reactions (Hofmann degradation, etc.) [18]. It is well known that quaternary ammonium salts are capable of alkylating various organic compounds. The above processes may be responsible for the formation of 3a-methyl derivative **VIII** and demethylated compound **IX**. The alkylation of 5-acetyl-hexahydropyrazolo[4,3-*c*]pyridines at the $N^1$ or bridgehead $C^{3a}$ atom was reported in [23]. 3a-Methyl derivative **VIII** could be formed via both autoalkylation of initial pyrazolopiperidine **IIa** at the $C^{3a}$ atom of the enol form and alkylation of pyrazolotetrahydropyridine **VI** possessing an enamine fragment.

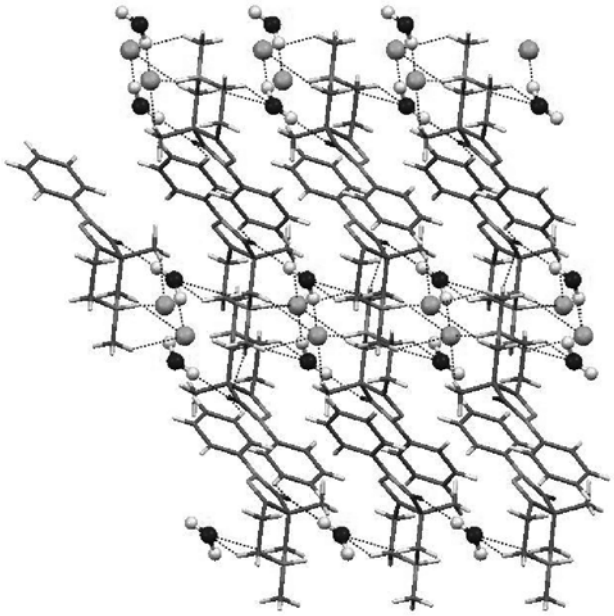

**Fig. 19.** A fragment of the three-dimensional network formed in the crystal structure of hydrochloride hydrate **XIII** via hydrogen bonds of various types.

Although zwitterionic structures **III** and **IV** should favor alkylation and ring contraction processes in pyrazolopiperidine **IIa**, it is quite difficult to propose a feasible scheme for the formation of phenylhydrazones **VII** and **IX** with account taken of recyclization of one fragment and opening of the other and even more so with loss of a $C_2H_2$ fragment. However, assuming active participation of oxygen and water, as was noted for analogous processes [20], the following hypothetic scheme may be supposed.

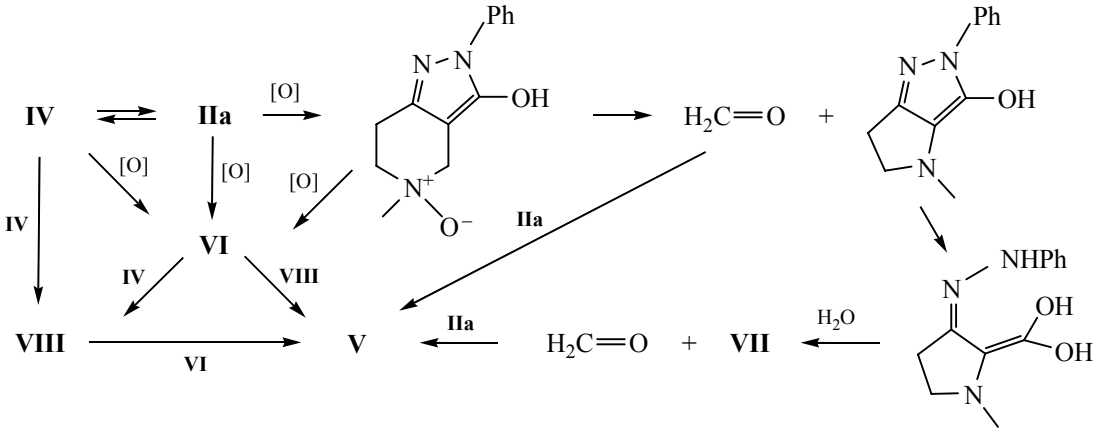


The different stabilities of previously described 5-acyl, 5-aryl, 5-(pyridinylmethyl), and even benzyl derivatives of 3,3a,4,5,6,7-hexahydro-2*H*-pyrazolo-[4,3-*c*]pyridin-3-one [24] and 5-alkyl-2-aryl derivatives synthesized by us are likely to be related to different basicity centers in their molecules. Introduction of such acceptor groups as acyl, aryl, or pyridinylmethyl strongly reduces the basicity of the piperidine nitrogen atom (or makes the other center more basic), so that the formation of zwitterionic structure like **III** or **IV** becomes improbable. We believe that the absence of quaternary ammonium group reduces the probability for analogous transformations of 5-acyl-, 5-aryl-, and 5-(pyridinylmethyl)-3,3a,4,5,6,7-hexahydro-2*H*-pyrazolo[4,3-*c*]-pyridin-3-ones.

## EXPERIMENTAL

The $^1$H and $^{13}$C NMR spectra were recorded on Bruker Avance-600 (600 MHz) and Avance-400 spectrometers (400 MHz for $^1$H) using the solvent signals as reference. The IR spectra were measured on a Bruker Vector-22 instrument from samples dispersed in mineral oil or pelleted with KBr (the difference in the position of bands did not exceed 1–2 cm$^{-1}$). The melting points were determined on Boetius PTP melting point apparatuses. The mass spectra (electron impact) were obtained on a Finnigan Trace MS instrument.

The X-ray diffraction data for single crystals of compounds **V**–**VII** and **XIII** were obtained at the Joint Spectral and Analytical Center for Physicochemical Studies of Structure, Properties, and Composition of Substances and Materials of the Arbuzov Institute of Organic and Physical Chemistry. Experiments were carried out on a NONIUS B.V. CAD-4 automated diffractometer (20°C, Cu$K_\alpha$ radiation, λ 1.54184 Å, graphite monochromator) for **V1** and on a Bruker Smart Apex II CCD automatic diffractometer (Mo$K_\alpha$ radiation, λ 0.71073 Å, graphite monochromator) at 23°C for **V2**, **VI**, and **VII** and at –123°C for **XIII**. No reduction of intensity of control reflections was observed during the data acquisition, and corresctions for absorption were applied. All the examined compounds formed colorless prismatic crystals in rhombic (**V2**) or monoclinic crystal system (all other compounds). Table 6 contains the crystallographic parameters of **V**–**VII** and **XIII** and parameters of X-ray diffraction experiments and structure refinement. Selected geometric parameters of molecules **V**–**VII** and **XIII** are given in Tables 2 and 3.

The structures were solved by the direct method using SIR [25] and SHELXS [26] and were refined ny the least-squares procedure first in isotropic and then in anisotropic approximation using SHELXL [26]. Hydrogen atoms in the amino groups and water molecule were visualized from the difference electron density maps, and their positions were refined in isotropic approximation. The coordinates of the other

**Table 6.** Crystallographic parameters of compounds **V**–**VII** and **XIII** and conditions of X-ray diffraction experiments

| Parameter | **V1** | **V2** | **VI** | **VII** | **XIII** |
|---|---|---|---|---|---|
| Space group | *C* 2/*c* | $P2_12_12$ | $P\,2_1/c$ | $P\,2_1/c$ | $P\,2_1/c$ |
| Formula | $C_{27}H_{30}N_6O_2$ | $C_{27}H_{30}N_6O_2$ | $C_{13}H_{13}N_3O$ | $C_{11}H_{13}N_3O$ | $C_{14}H_{18}N_3O^{+\cdot}\,Cl^-\,H_2O$ |
| Unit cell parameters | *a* 22.865(8)<br>*b* 17.586(8 )<br>*c* 16.531(6) Å<br>β 131.72(3)° | *a* 11.670(1)<br>*b* 12.354(1)<br>*c* 17.486(1) Å | *a* 10.4945(3)<br>*b* 10.1283(3)<br>*c* 21.3515(7) Å<br>β 95.000(2)° | *a* 6.516(2)<br>*b* 13.521(4)<br>*c* 11.582(3) Å<br>β 94.477(3)° | *a* 11.964(2)<br>*b* 11.175(2)<br>*c* 11.628(2) Å<br>β 111.067(2)° |
| Unit cell volume, $Å^3$ | 4962(3) | 2520.8(4) | 2260.9(1) | 1017.4(5) | 1450.8(4) |
| *Z* | 8 | 4 | 8 | 4 | 4 |
| *M* | 470.57 | 470.57 | 227.26 | 203.24 | 297.78 |
| $d_{calc}$, $g/cm^3$ | 1.260 | 1.240 | 1.335 | 1.327 | 1.363 |
| Absorption coefficient, $cm^{-1}$ | 6.60 | 0.81 | 0.88 | 0.89 | 2.69 |
| *F*(000) | 2000 | 1000 | 960 | 432 | 632 |
| X-Ray radiation, λ, Å | 1.54184 | 0.71073 | 0.71073 | 0.71073 | 0.71073 |
| θ range | 3.61–74.19 | 2.85–27.97 | 2.61–32.05 | 2.32–28.41 | 1.82–28.80 |
| *hkl* ranges | $0 \le h \le 28$,<br>$0 \le k \le 21$,<br>$-20 \le l \le 15$ | $-15 \le h \le 15$,<br>$-14 \le k \le 16$,<br>$-22 \le l \le 22$ | $-14 \le h \le 14$,<br>$-12 \le k \le 15$,<br>$-29 \le l \le 26$ | $-8 \le h \le 8$,<br>$-17 \le k \le 17$,<br>$-15 \le l \le 15$ | $-16 \le h \le 15$,<br>$-15 \le k \le 14$,<br>$-15 \le l \le 15$ |
| Total number of reflections | 5141 | 18726 | 11454 | 8833 | 21353 |
| $R_{int}$ | 0.0467 | 0.0949 | 0.0225 | 0.0647 | 0.0380 |
| Number of independent reflections with $I > 2\sigma(I)$ | 4138 | 2695 | 3553 | 891 | 2946 |
| Divergence factors for reflections with $I > 2\sigma(I)$ | *R* 0.0425,<br>$R_w$ 0.1192 | *R* 0.0744,<br>$R_w$ 0.1803 | *R* 0.0745,<br>$R_w$ 0.2012 | *R* 0.0576,<br>$R_w$ 0.1286 | *R* 0.0543,<br>$R_w$ 0.1305 |
| Goodness of fit | 1.008 | 0.958 | 1.036 | 0.915 | 1.047 |
| Number of variables | 318 | 317 | 303 | 141 | 192 |
| Maximum and minimum residual electron density peaks, $\bar{e}/Å^3$ | 0.204,<br>–0.140 | 0.544,<br>–0.176 | 0.782,<br>–0.680 | 0.148,<br>–0.181 | 0.449,<br>–0.363 |

hydrogen atoms were calculated on the basis of stereochemical considerations and were refined according to the riding model.

The data were acquired and edited, and the unit cell parameters were refined with the aid of MolEN [27] and APEX2 packages [28]. All calculations were performed using WinGX [29], intermolecular interactions were analyzed by PLATON [30], and the molecular structures were plotted using Mercury [31].

The coordinates of atoms in structures **V**–**VII** and **XIII** and their temperature factors were deposited to the Cambridge Crystallographic Data Centre (entry nos. CCDC 942 105–942 109, respectively).

**3a,3a′-Methylenebis(5-methyl-2-phenyl-3,3a,4,5,6,7-hexahydro-2*H*-pyrazolo[4,5-*c*]pyridin-3-one) (V).** *a*. A mixture of 5.0 g (0.292 mol) of methyl 1-methyl-4-oxopiperidine-3-carboxylate (**Ia**) and 3.16 g (0.292 mol) of freshly distilled phenylhydrazine in 25 mL of methanol was heated for 10 min under reflux and was then left overnight at room temperature. The precipitate was filtered off and washed on a filter with cold methanol to isolate 1.9 g (27.6%) of **V** as color-

less crystals. Recrystallization from carbon tetrachloride gave fine colorless crystals with mp 189–191°C (decomp., PTP), 185–188°C (decomp., Boetius). In both cases recrystallization was observed in the temperature range from 162 to 168°C. The product is soluble in acetone, DMSO, MeCN, and $CH_2Cl_2$, and poorly soluble in $CCl_4$. Samples of **V** obtained by recrystallization from $CCl_4$, MeOH, *i*-PrOH, acetone, or MeCN had identical IR spectra. IR spectrum (KBr), ν, $cm^{-1}$: 3065, 2972, 2942, 2894, 2856, 2789, 2716, 1698, 1688, 1619, 1596, 1497, 1453, 1392, 1366, 1347, 1285, 1251, 1213, 1197, 1171, 1135, 1114, 1088, 1038, etc. $^1$H NMR spectrum ($CCl_4$), δ, ppm (*J*, Hz): 7.20 d (4H, *o*-H, $^3J$ = 8.0), 6.85 t (4H, *m*-H, $^3J$ = 8.0), 6.69 t (2H, *p*-H, $^3J$ = 8.0), 2.58–2.74 m (8H, 4-$H_{eq}$, 6-$H_{eq}$, 7-$H_{eq}$, 3a-$CH_2$), 2.01 m (2H, 4-$H_{ax}$), 1.99 s (6H, NMe), 1.61 m (2H, 6-$H_{ax}$, 7-$H_{ax}$). $^{13}$C NMR spectrum ($CCl_4$), $\delta_C$, ppm: 172.23 (C=O), 162.79 (C=N), 137.70 ($C^i$), 127.98 ($C^m$), 124.03 ($C^p$), 118.03 ($C^o$), 64.29 ($C^4$), 57.60 ($C^6$), 54.16 ($C^{3a}$), 45.06 (NMe), 36.97 (3a-$CH_2$), 27.98 ($C^7$). Found, %: C 68.63; H 6.46; N 17.89. $C_{27}H_{30}N_6O_2$. Calculated, %: C 68.92; H 6.27; N 17.85. Mass spectrum: *m*/*z* 470. Calculated: *M* 470.537.

*b*. The mother liquor was combined with the methanol washings, and 3 mL of 40% aqueous formaldehyde was added. Extensive separation of crystals started immediately. After 0.5 h, the crystals were filtered off and washed with cold methanol to isolate an additional portion, 4.06 g, of **V** as white crystals. The IR spectra of both samples were identical.

*c*. Pyrazolopiperidine **IIa**, 3.0 g, synthesized from keto ester **Ib** and phenylhydrazine in methanol at 15–20°C [1], was recrystallized was dissolved in 30 mL of boiling 96% ethanol. The solution was cooled and kept for two days at room temperature, and the precipitate was filtered off, washed on a filter with ethanol, and dried. Yield 1.31 g. According to the TLC data, the product was identical to samples prepared as described in *a* and *b*.

**3a,3a′-Methylenebis(5-methyl-2-phenyl-3,3a,4,5,6,7-hexahydro-2*H*-pyrazolo[4,5-*c*]pyridin-3-one) dihydrochloride (V)·2HCl.** Dry hydrogen chloride was passed through a solution of **V** in methylene chloride. The precipitate was filtered off and recrystallized from methanol. The product is readily soluble in water and DMSO. IR spectrum (KBr), ν, $cm^{-1}$: 3424 v.br, 3106, 3061, 3012, 2943, 2665, 2585, 2544, 2450, 1711, 1630, 1595, 1497, 1462, 1429, 1405, 1359, 1323, 1273, 1236, 1138, 1094, 1065. Found, %: C 59.98; H 5.88; Cl 12.81; N 15.29. $C_{27}H_{30}N_6O_2\cdot 2HCl$. Calculated, %: C 59.67; H 5.93; Cl 13.05; N 15.46.

**5-Methyl-2-phenyl-3,5,6,7-tetrahydro-2*H*-pyrazolo[4,5-*c*]pyridin-3-one (VI).** A mixture of 2.0 g of pyrazolopiperidine **IIa** and 50 mL of anhydrous propan-2-ol was heated under reflux until complete dissolution. The solution was filtered while hot and was left to stand for 3 days at room temperature. The crystals were filtered off, washed with propan-2-ol, and dried. According to the IR and TLC data, the product (0.75 g, white fine crystals) was compound **V**. The mother liquor was evaporated under reduced pressure, and the residue, a dark thick oily material, was dissolved in a minimum amount of acetone. The solution was left overnight, and the crystals were filtered off and recrystallized once more from acetone. Yield of **VI** 0.15 g (7.6%), light brown needles, mp 197–198°C (decomp.). IR spectrum (KBr), ν, $cm^{-1}$: 3115, 3038, 2963, 2852, 2808, 1662, 1620, 1593, 1556, 1523, 1488, 1457, 1432, 1415, 1349,1326, 1249, 1202, 1178, 1158, 1119, 1091, 1063, 1041, 1020. $^1$H NMR spectrum ($CDCl_3$), δ, ppm (*J*, Hz): 7.98 d (2H, *o*-H, *J* = 7.7), 7.71 s (1H, 4-H), 7.36 t (2H, *m*-H, *J* = 7.5), 7.09 t (1H, *p*-H, *J* = 7.4), 3.50 t (2H, $CH_2$, *J* = 7.4), 3.17 s (3H, NMe), 2.86 t (2H, $CH_2$, *J* = 7.4). $^{13}$C NMR spectrum ($CDCl_3$), $\delta_C$, ppm: 163.25 ($C^3$), 150.27 ($C^4$), 144.85 ($C^{7a}$), 139.86 ($C^i$), 128.59 ($C^m$), 123.75 ($C^p$), 118.73 ($C^o$), 101.70 ($C^{3a}$), 49.13 ($C^6$), 44.04 ($NCH_3$), 22.94 ($C^7$). Found, %: C 68.87; H 5.86; N 18.28. $C_{13}H_{13}N_3O$. Calculated, %: C 68.71; H 5.77; N 18.48.

**Transformation of pyrazolopiperidine IIa in boiling methanol.** A solution of 2.3 g ( 0.01 mol) of pyrazolopiperidine **IIa** in 20 mL of methanol was heated for 4 h under reflux, evaporated to a volume of 5 mL, and left overnight. The crystals were filtered off and washed with cold methanol to isolate 0.6 g of compound **V** which was identical to samples obtained in other ways.

The filtrate and the washings were combined and mixed with 10 g of silica gel. After a time, silica gel was separated and dried under reduced pressure at 40–50°C. The dry powder was placed into a narrow Schott funnel and slowly washed with 100 mL of methylene chloride. Removal of the solvent gave 0.6 g of a yellow thick oily substance. According to the $^1$H and $^{13}$C NMR data, it contained approximately equal amounts of compounds **VIII** and **IX** and a small impurity of unidentified product.

**3a,5-Dimethyl-2-phenyl-3,3a,4,5,6,7-hexahydro-2*H*-pyrazolo[4,3-*c*]pyridin-3-one (VIII).** $^1$H NMR spectrum ($CDCl_3$), δ, ppm (*J*, Hz): 7.92 (2H, *o*-H), 7.39 (2H, *m*-H), 7.17 (1H, *p*-H), 3.13 m (1H, 6-H), 2.96 m (1H, 4-H), 2.73 m and 2.61 m (1H each, 7-H), 2.35 s (3H, NMe), 2.08 m (1H, 6-H), 2.05 m (1H, 4-H), 1.53 s (3H, 3a-Me). $^{13}$C NMR spectrum ($CDCl_3$), $\delta_C$, ppm: 175.44 ($C^3O$), 165.57 ($C^7$), 138.23 ($C^i$), 128.76 ($C^m$), 124.84 ($C^p$), 118.63 ($C^o$), 62.37 ($C^4$), 57.32 ($C^6$), 51.50 ($C^{3a}$), 45.09 (NMe), 27.39 ($C^7$), 18.56 (3a-Me).

**Methyl 3-(2-phenylhydrazinylidene)-4,5-dihydro-3*H*-pyrrole-2-carboxylate (IX).** $^1$H NMR spectrum ($CDCl_3$), δ, ppm (*J*, Hz): 7.32 (1H, NH), 7.27 (2H, *m*-H), 7.12 (2H, *o*-H), 6.93 (1H, *p*-H), 4.28 (2H, 5-H), 3.97 (3H, OMe), 2.61 (2H, 4-H). $^{13}$C NMR spectrum ($CDCl_3$), $\delta_C$, ppm: 163.84 ($C^2$), 162.71 (C=O), 145.66 ($C^3$), 143.70 ($C^i$), 129.22 ($C^m$), 121.46 ($C^p$), 113.61 ($C^o$), 58.02 ($C^5$), 52.57 ($OCH_3$), 25.12 ($C^4$).

The sorbent was then eluted with methylene chloride–methanol (10 : 1). The solvent was removed to obtain 0.86 g of a light brown oily substance which was dissolved in 5 mL of hot acetone. After cooling, the precipitate was filtered off and recrystallized once more from acetone. Yield of **VI** 0.2 g, light brown crystals whose IR spectrum was identical to that given above.

A small amount of gaseous hydrogen chloride was passed through the mother liquor after separation of pyrazolotetrahydropyridine **VI**. After some time, two kinds of crystals separated and were sorted out from each other manually. The colorless crystals underwent recrystallization at 225–230°C and gradually decomposed above 300°C. Their structure was determined by X-ray analysis as hydrochloride hydrate **VIII**·HCl·$H_2O$ (**XIII**).

The yellowish crystals flowed on heating above 140°C and gradually decomposed. According to the X-ray diffraction data, these crystals were aslo hydrochloride **XIII** solvated with methanol.

**(3*E*)-1-Methyl-3-(2-phenylhydrazinylidene)pyrrolidin-2-one (VII).** A mixture of 1.0 g (0.0018 mol) of sesquihydrochloride **X** (2**IIa**·3HC), 20 mL of a saturated solution of potassium carbonate, and 10 mL of methylene chloride was shaken in a separatory funnel until complete dissolution. The mixture was allowed to settle down, and it divided into three layers. The bottom aqueous salt layer was discarded, the middle layer was a solution of dihetarylmethane **V** in methylene chloride, and the upper layer was a light yellow low-mobile oily substance which slowly crystallized. The resulting powder was treated with 15 mL of methanol, and about 0.05 g (6%) of light yellow crystals of **VII** separated from the solution after some time. mp 248–249°C; published data [17]: mp 237–239°C (decomp., from 2-methoxyethanol). After storage for several years, crystals of **VII** were transformed into a red tarry material. $^1$H NMR spectrum, δ, ppm (*J*, Hz): in DMSO-$d_6$: 9.49 s (1H, NH), 7.22 t (2H, *m*-H, *J* = 7.3), 7.17 d (2H, *o*-H, *J* = 7.3), 6.80 t (1H, *p*-H, *J* = 7.3), 3.48 t (2H, 5-H, *J* = 6.6), 2.86 s (3H, NMe), 2.72 t (2H, 4-H, *J* = 6.6); in $CDCl_3$: *E* isomer: 7.50 s (1H, NH), 7.10 d (2H, *o*-H, *J* = 7.3), 6.95 t (2H, *m*-H, *J* = 7.3), 6.88 t (1H, *p*-H, *J* = 7.3), 3.54 t (2H, 5-H, *J* = 6.6), 2.93 s (3H, NMe), 2.68 t (2H, 4-H, *J* = 6.6); *Z* isomer: 12.04 s (1H, NH), 7.32–7.23 m (5H, Ph), 3.59 t (2H, 5-H, *J* = 6.6), 3.03 s (3H, NMe), 2.73 t (2H, 4-H, *J* = 6.6). $^{13}$C NMR spectrum (DMSO-$d_6$), $\delta_C$, ppm: 164.38 ($C^2$), 145.08 ($C^i$), 138.41 ($C^3$), 129.02 ($C^m$), 120.00 ($C^p$), 113.15 ($C^o$), 44.28 ($C^5$), 30.07 (NMe), 21.82 ($C^4$). IR spectrum (mineral oil), ν, $cm^{-1}$: 3278, 1678, 1660 pl, 1625, 1545, 1496, 1312, 1300, 1272. Mass spectrum: *m*/z 203.

## ACKNOWLEDGMENTS

The authors thank Prof. Sh.K. Latypov for his participation in structural studies of the described compounds by NMR spectroscopy and R.Z. Musin for recording the mass spectra.

This study was performed under financial support by the Russian Foundation for Basic Research and by the Academy of Sciences of Tatarstan Republic (project no. 12-03-97042r_povolzh'e_a).

## REFERENCES

1. Buzykin, B.I., Gubaidullin, A.T., Nabiullin, V.N., and Safina, A.F., *Russ. J. Gen. Chem*., 2014, vol. 84, no. 3, p. 531.
2. Nabiullin, V.N., Gubaidullin, A.T., Buzykin, B.I., and Litvinov, I.A., Abstracts of Papers, *III Natsional'naya Krystallokhimicheskaya Konferentsiya* (IIIrd National Crystallochemical Conf.), Chernogolovka, 2003, p. 94.
3. Buzykin, B.I. and Nabiullin, V.N., Abstracts of Papers, *IV Vserossiiskii simpozium po organicheskoi khimii "Upadok ili vozrozhdenie"* (IVth All-Russian Symp. on Organic Chemistry "Decadence or Renaissance"), Moscow: Mosk. Gos. Univ.– Chembridg Corporation, 2003, p. 24.

4. Kharlamov, S.V., Balandina, A.A., Azancheev, N.M., Latypov, Sh.K., Nabiullin, V.N., and Buzykin, B.I.,, Abstracts of Papers, *IV Vserossiiskaya konferentsiya "Novye dostizheniya YaMR v strukturnykh issledovaniyakh"* (IVth All-Russian Conf. "New Advances of NMR in Structural Studies"), Kazan: Kazan. Gos. Univ., 2005, p. 92.
5. Buzykin, B.I., *Ezhegod. Inst. Org. Fiz. Khim. im. A.E. Arbuzova*, Kazan, 2007, p. 25.
6. Nabiullin, V.N., Buzykin, B.I., and Gubaidullin, A.G., Abstracts of Papers, *Vserossiiskaya nauchnaya konferentsiya "Uspekhi sinteza i kompleksoobrazovaniya"* (All-Russian Scientific Conf. "Advances in Synthesis and Complex Formation"), Moscow: Ross. Univ. Druzhby Narodov, 2011, p. 188.
7. Buzykin, B.I., Nabiullin, V.N., Gubaidullin, A.T., and Kharlamov, S.V., *Russ. J. Gen. Chem*., 2013, vol. 83, no. 11, p. 2084.
8. Derome, A.E., *Modern NMR Techniques for Chemistry Research*, Oxford: Pergamon, 1987.
9. Atta-ur-Rahman, *One and Two Dimensional NMR Spectroscopy*, Amsterdam: Elsevier, 1989.
10. Stott, K., Stonehouse, J., Keeler, J., Hwang, T.L., and Shaka, A.J., *J. Am. Chem. Soc*., 1995, vol. 117, no. 14, p. 4199.
11. Price, W.S., *Concepts Magn. Reson*., 1997, vol. 9, no. 5, p. 299.
12. Allen, F.H., Kennard, O., Watson, D.G., Brammer, L., Orpen, A.G., and Taylor, R., *J. Chem. Soc., Perkin Trans. 2*, 1987, no. 12, p. S1.
13. Buzykin, B.I., Cherepinskii-Malov, V.D., Litvinov, I.A., Gazetdinova, N.G., and Struchkov, Yu.T., *Izv. Akad. Nauk SSSR, Ser. Khim*., 1982, no. 6, p. 1306.
14. Vickery, B., Willey, G.R., and Drew, M.G.B., *J. Chem. Soc., Perkin Trans. 2*, 1981, no. 1, p. 155.
15. Litvinov, I.A., Struchkov, Yu.T., Bystrykh, N.N., and Buzykin, B.I., *Khim. Geterotsikl. Soedin*., 1982, no. 8, p. 1100.
16. Kitaigorodskii, A.I., *Molekulyarnye krystally* (Molecular Crystals), Moscow: Nauka, 1971.
17. Eiligsfeld, H., Seefelder, M., and Weidinger, H., *Chem. Ber*., 1963, vol. 96, no. 11, p. 2899.
18. Sweeney, J.B., Tavassoli, A., Carter, N.B., and Hayes, J.F., *Tetrahedron*, 2002, vol. 58, no. 51, p. 10113.
19. Mageswaran, S., Ollis, W.D., and Sutherland, I., *J. Chem. Soc., Perkin Trans. 1*, 1981, no. 7, p. 1953.
20. Golubev, V.A. and Sen', V.D., *Russ. Chem. Bull., Int. Ed*., 2009, vol. 58, no. 9, p. 1824.
21. Voskresenskii, L.G., Borisova, T.N., Ovcharov, M.V., Kulikova, L.N., Sorokina, E.A., Borisov, R.S., and Varlamov, A.V., *Chem. Heterocycl. Compd*., 2008, no. 12, p. 1510.
22. Voskresenskii, L.G., Borisova, T.N., Kamaletdinova, T.M., Titov, A.A., Listratova, A.V., and Varlamov, A.V., *Russ. Chem. Bull., Int. Ed*., 2010, vol. 59, no. 3, p. 647.
23. Pfeffer, K.-G., Brandt, P., Buge, A., Hahn, H.-J., Heeger, G., and Reppel, L., *Pharmazie*, 1977, vol. 32, no. 11, p. 676.
24. Alterburger, J.-M., Fossey, V., Illano, S., and Manette, G., FR Patent no. 2940652, 2010; *Chem. Abstr*., 2010, vol. 153, no. 145480.
25. Altomare, A., Burla, M.C., Camalli, M., Cascarano, G.L., Giacovazzo, C., Guagliardi, A., Moliterni, A.G.G., Polidori, G., and Spagna, R., *J. Appl. Crystallogr*., 1999, vol. 32, no. 1, p. 115.
26. Sheldrick, G.M., *SHELX-97. Programs for Crystal Structure Analysis (Release 97-2)*, Göttingen, Germany: Univ. of Göttingen, 1997.
27. Straver, L.H. and Schierbeek, A.J., *MOLEN. Structure Determination System, vol. 1. Program Description*, Nonius B.V., 1994.
28. *APEX2 (Version 2.1), SAINTPlus. Data Reduction and Correction Program (Version 7.31A, Bruker Advanced X-Ray Solutions*, Madison, Wisconsin, USA: Bruker AXS, 2006.
29. Farrugia, L.J., *J. Appl. Crystallogr*., 1999, vol. 32, no. 4, p. 837.
30. Spek, A.L., *J. Appl. Crystallogr*., 2003, vol. 36, no. 1, p. 7.
31. Macrae, C.F., Edgington, P.R., McCabe, P., Pidcock, E., Shields, G.P., Taylor, R., Towler, M., and van de Streek, J., *J. Appl. Crystallogr*., 2006, vol. 39, no. 3, p. 453.